FACTORS AFFECTING

BANDSAW TRACKING BEHAVIOR AND STABILITY

by

DARRELL C. WONG

B.A.Sc., The University of British Columbia, 1991

A THESIS SUBMITTED IN PARTIAL FULFILLMENT OF

THE REQUIREMENTS FOR THE DEGREE OF

MASTER OF APPLIED SCIENCE

in

THE FACULTY OF GRADUATE STUDIES

Department of Mechanical Engineering

We accept this thesis as conforming
to the required standard

THE UNIVERSITY OF BRITISH COLUMBIA

October 1996

In presenting this thesis in partial fulfilment of the requirements for an advanced degree at the University of British Columbia, I agree that the Library shall make it freely available for reference and study. I further agree that permission for extensive copying of this thesis for scholarly purposes may be granted by the head of my department or by his or her representatives. It is understood that copying or publication of this thesis for financial gain shall not be allowed without my written permission.

Department of MECHANICAL ENGINEERING

The University of British Columbia
Vancouver, Canada

Date OCTOBER 15/96

DE-6 (2/88)

Abstract

This theoretical and experimental study examines the tracking behavior and stability of bandsaw blades. Tracking describes the in-plane "front-to-back" motion of a bandsaw as it runs on the bandmill wheels. Bandsaw tracking stability returns the sawblade to its initial position after any in-plane side-to-side displacement caused by a cutting force. The tracking behavior and stability of the sawblade are determined by the geometry of the saw and bandmill wheels. Fourteen factors affect this geometry. They are the cutting force, wheel profile, tilt, cross line and coefficient of friction, and the saw backcrown, overhang, strain, tensioning, thickness, width, guides, rotational speed and temperature distribution. In practice, many of these factors are present at the same time.

A theoretical model is presented here that accurately and reliably predicts the behavior and stability of the band. This model incorporates and quantifies the tracking stability of cutting force, wheel profile and tilt, and band overhang, strain, thickness and width. Both the experimental and theoretical results show that wheel crown and overhang are the only true stability factors and that the other factors such as width and thickness only modify the stability of crown and overhang. It was also found that the detail of the wheel profile has a substantial effect on tracking stability and when wheel crown is combined with overhang, the tracking stability of overhang is improved. The model can now be applied to investigate different wheel crown profiles. It provides an important tool for the task of improving bandsaw cutting performance while at the same time reducing the required saw and bandmill maintenance.

TABLE OF CONTENTS

List of Figures

Acknowledgment

I would like to express my gratitude to those individuals and organizations who have supported this work. A special thank you to everyone in my family who enthusiastically supported my return to university. My wife Shelley for her love and patience, my mother Jane for her incredible dedication to raising my brothers and I, and my mother and father-in-law Elizabeth and Ted for their love and caring.

My work on this project was made possible by the financial support of the BC Science Council, Natural Science and Engineering Research Council of Canada (NSERC), Forintek Canada Corporation and MacMillan Bloedel Ltd. In particular, I would like to thank John Taylor and Jan Aune for supporting this work from the beginning.

Finally, I would like to thank my faculty sponsor, Gary Schajer, who was the key to my "tracking" back to university. Thank you for your encouragement, support and most of all, for your confidence in me.

Nomenclature

a	=	crown height adjustment factor
B_1, B_2, B_3, B_4	=	beam equation integration constants
b	=	band width
C_1, C_2, C_3, C_4	=	cylindrical shell equation integration constants
D, D_1, D_2	=	wheel diameters
d	=	overhang distance
dw / dy	=	overhang slope
dy / dx	=	band slope
d^2y / dx^2	=	band curvature
E	=	band material elastic modulus
F	=	lateral cutting force
front-to-back	=	in-plane band motion in the workpiece feed direction
$f(y), f_2(y), f_3(y), f_4(y)$	=	wheel profile function
H, J, k, η	=	equation constants
h	=	band thickness
I	=	band second moment of area
u	=	offset from crown center
L	=	band length between wheels
L_T	=	total circumferential band length
L_0	=	original band section length before it's wrapped around wheel

$M, M(z)$	=	bending moment
M_A	=	bending moment at wheel entry point A
P	=	uniform pressure between band and wheel
q	=	overhang coordinate
R	=	curvature radius of unwrapped wheel
R_A	=	band reaction force at wheel entry point A
r	=	wheel radial coordinate with the datum at wheel center
r_0	=	mean radius of profiled wheel
s	=	wheel width
T	=	band axial tensile force / span (strain force)
$V(d)$	=	shear force at wheel edge due to overhang
V_L	=	band longitudinal velocity
V_T	=	band transverse velocity across wheel
$w, w(y)$	=	curling of overhang
x	=	coordinate along length of band from wheel entry point A
Δx	=	incremental longitudinal movement or rotation of the band
y	=	coordinate perpendicular to band
$y(x)$	=	band position as a function of x
y_G	=	band position at wheel exit point G
z	=	wheel profile radial coordinate with datum at band centerline
$\gamma, \gamma_1, \gamma_2$	=	wheel taper angle
β	=	wheel tilt angle

ϕ, ϕ_A	=	band entry angle, top wheel band entry angle
ϕ_G	=	bottom wheel band exit angle
ϕ_S	=	Swift's steady state band entry angle
ν	=	band material Poisson's ratio
σ_0	=	base uniform stress in band from wheel profile
σ_x	=	longitudinal stress in band

1.0 Introduction

1.1 Background

Global competition demands that sawmill managers and maintenance personnel continue to pursue ways to improve lumber production quality and reduce operating costs. Each step in the overall log breakdown process is being examined to contribute to this goal [1,2]. Bandsaws are major machines in many mills, and they process large volumes of wood. Therefore, they are good targets for production quality improvements and operating cost reductions.

A bandsaw machine or bandmill consists of a continuous band traveling around two wheels as shown in figure 1.1. The preparation of the bandsaw can be a time consuming process which includes tensioning, leveling and sharpening of the sawblade [3]. The maintenance and set-up of the bandmill includes machining the surfaces of the wheels to a flat or crowned profile, setting the "strain" force to pull the sawblade firmly onto the wheels, and adjusting the position of the sawblade by setting the "tilt" angle between the axes of the top and bottom wheels.

The maintenance and set-up of the bandmill and bandsaw are performed with the goal of achieving good cutting performance at a high production rate while consuming a minimum amount of maintenance time. The dilemma is that typically an improvement in one operational area can only be achieved at the cost of another [4]. For example, good cutting performance

can be achieved through careful saw tensioning and lower production rates. Less maintenance time spent on tensioning and also higher production rates typically reduce cutting performance.

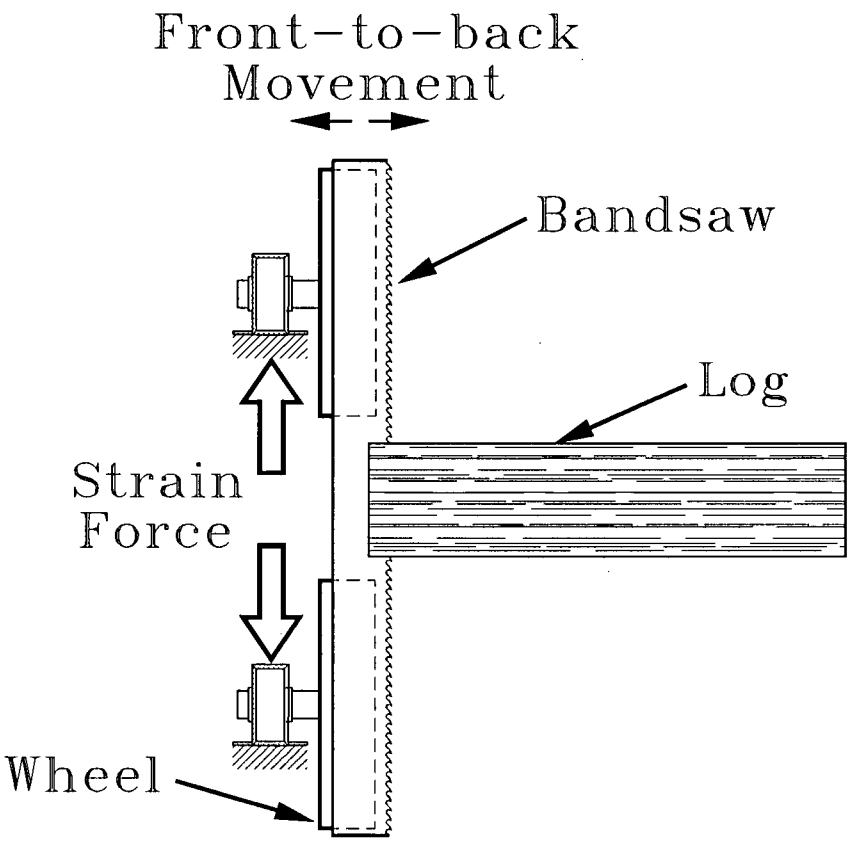

Figure 1.1: Bandsaw Machine and Sawblade

An understanding of bandsaw tracking may contribute to a solution to this dilemma. The term "tracking" describes the in-plane "front-to-back" movement of the saw as it runs between the wheels of a bandmill [5,6]. During sawing, the cutting forces create an in-plane bending moment and curvature along the length of the sawblade. As the sawblade rotates around the wheels the curvature creates an angle between the saw and bandmill wheel at the point where

the saw first contacts and moves onto the wheel. This angle is called the "entry angle" ϕ. The entry angle is a key quantity that describes tracking. It defines the ratio of the in-plane sideways speed of the saw relative to its longitudinal speed. When the entry angle is non-zero the sawblade is not perpendicular to the wheel axis. As a result, the sawblade moves sideways in a screw-like motion, with the entry angle corresponding to the thread angle of the screw. This sideways motion is tracking. When the entry angle is zero the saw is perpendicular to the wheel axis and as a result, it runs in a stable tracking position without any sideways motion.

The ability of a moving bandsaw to maintain its tracking position against the cutting forces that tend to push the saw off the wheels is referred to as tracking stability [6,7,8]. The sawblade relies on subtle details such as the bandmill wheel profile and saw overhang to generate a bending moment to counteract the moment created by the cutting forces. The balance between these moments determines the tracking displacement of the saw and it keeps the saw on the wheels without any direct mechanical constraint. A sawblade with a high tracking stability moves a small distance in response to a cutting force while one with a low stability moves a larger distance. Many other factors also contribute to the balancing moment including the saw tensioning, thickness and width and the bandmill strain and the wheel tilt angle.

It is generally believed that front-to-back movement of the sawblade impairs cutting accuracy and increases the wear on the bandmill wheels and sawblade. Therefore, a saw with a higher tracking stability that responds with minimum movement to the cutting force will improve

cutting accuracy without a penalty in production rate. An understanding of bandsaw tracking may also provide a means of reducing sawblade maintenance time by reducing the amount of tensioning required in sawblades.

Previous tracking studies have focused mainly on the stable tracking position of bandsaws. This is "steady state" tracking. In practice, this condition occurs when a bandsaw is idling between saw cuts. However, when a bandsaw is cutting, its tracking position is continually changing. This is "transient" tracking. Therefore, to maximize cutting accuracy and minimize equipment maintenance time, bandsaw transient tracking must also be examined. This study will extend the previous steady-state tracking analysis to include the general transient case.

1.2 Previous Work

Swift's [8] work in the 1930's on the steady state tracking of belts around pulleys was among the first systematic studies to be published on tracking. His theory modeled the portion of the belt between the wheels as a beam in bending with an applied axial tensile load. The bending moment was calculated by assuming the stress distribution across the sawblade matched the profile of the pulley. The steady state entry angle was determined from the end slope of the beam. Swift's theory includes the effects of the wheel taper and circular crown and the belt width and strain. Wheel tilt and cross line were also included in Swift's theory as adjustments to the beam boundary conditions.

Schajer [9] also did work on tracking when he developed a geometrical model of how a guided circular saws hunts on a rotating shaft. The mechanism of saw hunting is the same as that for belt tracking. Schajer described in detail the movement of the saw as it enters onto and moves around the shaft. He explained that at the instant when the saw enters onto the shaft, it appears that the saw and shaft will follow different paths but since they are in contact, the saw must follow the rotation of the shaft.

The effect of wheel crown profile on the tracking stability of belts was experimentally examined by Renner [10]. He showed that a pulley with a flat center section and steeply curved edges has a higher tracking stability than a pulley with a center peak that gradually slopes towards the edges. In addition, he also showed that a band mounted on the pulley with the flat center section has a more uniform stress distribution across its width.

Sugihara [6] published some of the first work on the tracking of bandsaw blades. He theorized that the bending moment in the sawblade determined its tracking behavior. His work focused on the bending moments created by the cutting force, saw strain, saw width, wheel tilt and overhang. Like Swift, Sugihara modeled the band between the wheels as a beam under an axial tensile load. The cutting force was included as a concentrated force at the center of the beam. Saw overhang of a flat wheel was modeled as a cylindrical shell with a uniform line force and moment on one edge and the other edge free. The line force and moment were determined from the assumption that the bandmill wheel behaves as a beam on

an elastic foundation with the strain applied as a uniform pressure across the wheel. They are calculated by balancing the force and moment acting on the wheel edge.

Taylor [11] extended the work done by Sugihara. He developed theoretical models for the bending moments created by backcrown, tensioning and wheel crown and extended Sugihara's work on the bending moments generated by wheel tilt and overhang. Taylor's cylindrical shell theory of saw overhang modeled the flat wheel as a rigid body and included the effects of saw tensioning and anticlastic curvature.

Chardin [12] began the first of many experimental studies of bandsaw tracking that included coarse measurements of transient tracking but focused mainly on six factors that affect an industrial saw's overhang. It was found in this study that flat wheels were more stable than crowned wheels. This comparison will also be performed here in section 5. It was also found that tensioning and the coefficient of friction between the sawblade and wheel had little effect on the overhang. Wheel tilt caused the saw to track from the higher to the lower portion of the wheel axis. When an out of plane (lateral) load was applied to one edge of the saw or the edge was heated, the saw tracked in-plane from the loaded or heated edge towards the opposite edge. An in-plane load applied to the edge of the saw in the feed direction caused the saw to track in the same direction. Chardin also noted that the transient tracking caused by an in-plane load or feed force followed an inverse exponential relationship with the longitudinal movement of the saw.

Chardin [7] followed up the industrial studies with laboratory experiments on a metal band or a saw with no teeth. The previous experiments on the industrial bandmill were repeated reaffirming most of the initial findings except it was found that highly tensioned saws were more stable than untensioned saws. The effects of strain, thickness, width and wheel size on the saw's overhang were also examined. It was found that strain increased the stability of the band while the thickness and width had little effect. The tracking stability of a double cut bandmill with 8' wheels was found to be higher than a single cut resaw with 5' wheels.

Chardin and Sales [13] then performed a laboratory study confirming the results from Chardin's earlier laboratory experiments as well as examining the combined effects of wheel size, tensioning and strain on band tracking stability. It was found that typically a minimum amount of tensioning was required for maximum tracking stability but that tensioning beyond this amount provided no additional benefit.

Sales, Guitard, Fournier and Garin [14] also performed experiments on a industrial bandmill and a sawblade with teeth. The effect of edge heating, backcrown and the combined effects of strain, tensioning and flat / crowned wheels on tracking stability were examined. As found earlier by Chardin, heating one edge of the saw caused it to track in the direction of the opposite edge and strain increased the stability of the saw. It was also found that typically tensioned saws were more stable on flat wheels except for highly tensioned and untensioned saws which were more stable on crowned wheels. When the tracking movement was large,

crowned wheels were found to be better than flat wheels at preventing the sawblade from coming off the wheels.

Rivat, Sales, and Martin [15] also did laboratory experiments using more accurate equipment to examine the effect of wheel tilt, strain and longitudinal velocity on the band's overhang. Confirming Chardin's findings, it was found that wheel tilt caused the band to track from the higher down towards the lower portion of the wheel axis and that strain reduced the overhang. It was also found that the longitudinal blade velocity decreased the overhang.

1.3 Objectives and Scope

The objective of this research study is to develop a comprehensive theoretical model of bandsaw tracking including steady state and the more general transient tracking. The four steps required to achieve this objective are:

1. Apply the tracking mechanism identified by Swift [8] and Schajer [9] to bandsaw blades.
2. Isolate the bandsaw tracking factors identified by Chardin, Fournier, Garin, Guitard, Rivat, Sales, Sugihara and Swift [6,7,8,12,13,14,15]. Determine the tracking effect of these factors and place them into a logical framework.
3. Develop a theoretical tracking model that incorporates both the steady state and the transient tracking behavior of the sawblade. Swift's steady state tracking model of wheel taper, band thickness, width and strain will be developed into a basic model for transient tracking. Next, Swift's wheel tilt theory will be incorporated. Swift's and Taylor's [8,11]

wheel crown bending theory will be incorporated after it is extended to include more general shapes. Sugihara's and Taylor's cylindrical shell model of the sawblade overhang will also be developed for transient tracking. Finally, the initial beam theory will be extended to include Sugihara's model of the cutting force.

4. Test and experimentally verify the accuracy of the theoretical model on a table top bandmill model and metal band. Detailed measurements will be made of the band's in-plane side-to-side tracking position relative to its longitudinal movement.

Beyond these objectives, the theoretical model will be utilized to determine which tracking factors have the most significant effect on bandsaw tracking stability. Machine and sawblade set-up factors that determine cutting accuracy and equipment maintenance requirements will be given special attention. A particular area of interest is the possibility of improving the bandmill wheel profile to increase tracking stability and reduce the amount of saw tensioning needed. This would allow the saw strain and saw stiffness to be increased and may also reduce the frequency of fatigue cracks in the sawblade. This change has the attractive potential of improving cutting accuracy at the same time as reducing bandmill wheel wear and sawblade maintenance requirements.

2.0 Bandsaw Tracking Mechanism

The tracking or in-plane "front-to-back" movement of a bandsaw is determined by the geometries of the wheels and sawblade at the point where the saw first contacts ("enters") the wheel [16,17]. This tracking has two phases, transient and steady state. Transient tracking is the more general case during which both the side-to-side position and tracking speed of the band are continuously changing. After a few band rotations, the sideways tracking speed typically converges to a steady state value. This is called steady state tracking.

2.1 Tracking Movement

Bandsaw tracking movement occurs continuously and simultaneously around the entire saw as it rotates on the wheels. The direction and rate of movement of the saw is determined by saw's angle at the point where it first enters onto the wheel.

Mechanism of Tracking Movement

To illustrate the mechanism of bandsaw tracking movement, consider the straight band running on the flat (cylindrical) wheel shown in figure 2.1. In this simple case, the longitudinal force on the band, commonly called "strain", is evenly distributed across the width of the band. As a result, there is no bending or curvature, and the band remains straight and perpendicular to the wheel axis. Consider the instant when a point on the band first contacts the wheel at A. After contact, there is assumed to be no slip between the band and wheel.

Therefore, the band is constrained to follow the rotational path of the wheel. Here, the path of the band and the path of the wheel coincide because they are both destined for point B. Therefore, after a quarter or more turns of the wheel, the side-to-side position of the band on the wheel remains unchanged.

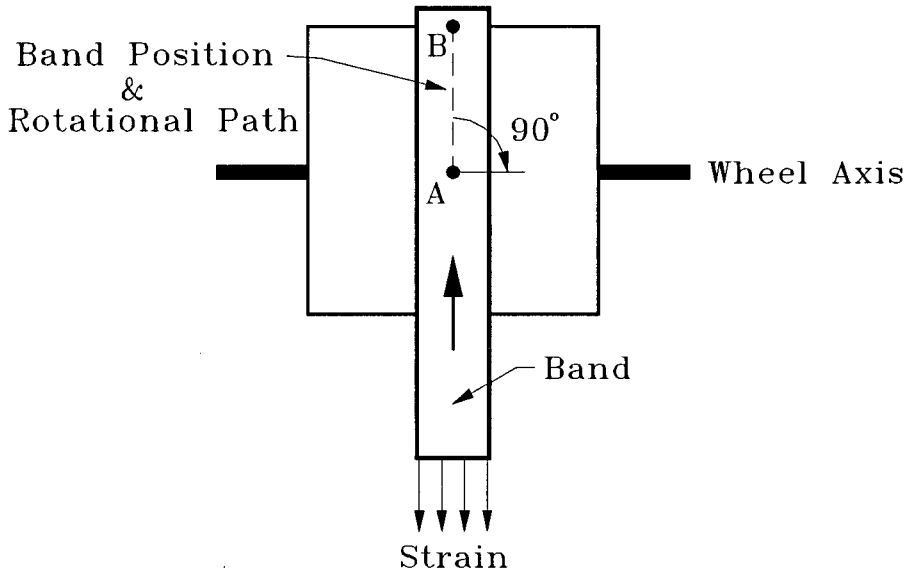

Figure 2.1: Flat Wheel Tracking

Now consider the initially straight band tracking on a tapered (conical) wheel shown in figure 2.2. The tapered wheel applies the strain unevenly to the band, resulting in a bending moment and a slight curve in the band [8]. The band axis is no longer perpendicular to the wheel axis. Consider the instant when a point on the band first contacts the wheel at A. At this instant, the path of the band appears destined for point B. However, point A on the wheel follows a path perpendicular to the rotational axis and is destined for point C. Since there is no slip between the band and the wheel, the band moves up the taper following the rotation of the

wheel [9]. Therefore, after a quarter turn the band has shifted sideways towards the wider side of the taper, as shown in figure 2.2.

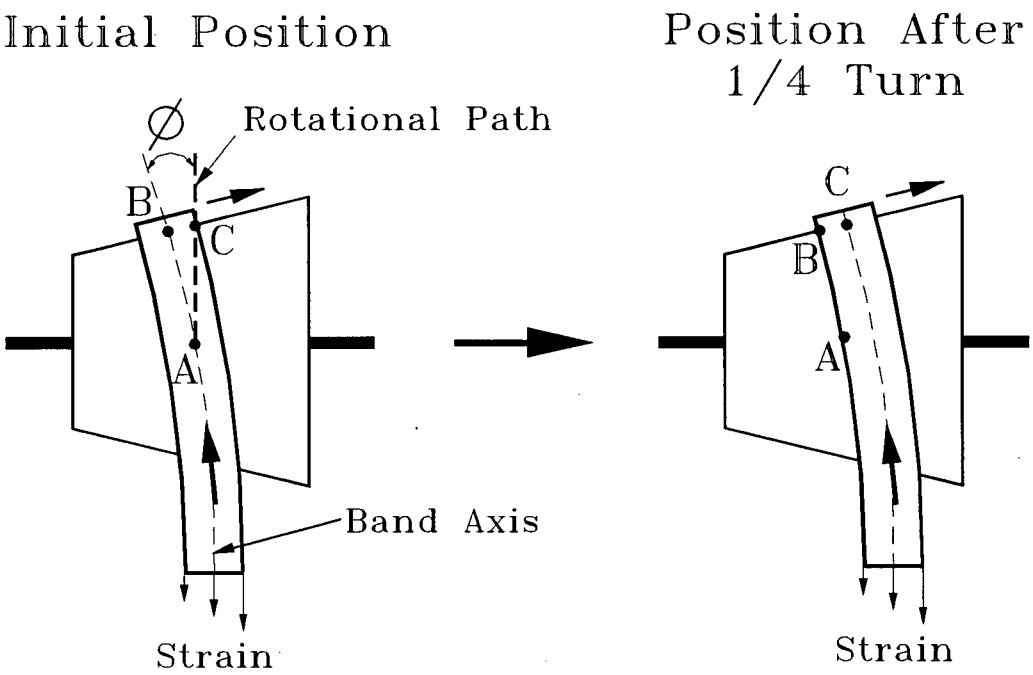

Figure 2.2: Tapered Wheel Tracking

Four basic concepts are important when considering band tracking movement. They are:

1. A bending moment creates a curvature along the length of the band.
2. Tracking occurs when the band rotational path is not perpendicular to the wheel axis at the point where the band first contacts ("enters") the wheel. The resulting perpendicular angle between the band axis and the wheel axis is called the "entry angle" ϕ. Figures 2.2 and 2.3 illustrate this angle.

3. The band tracking speed V_T depends proportionally on the entry angle ϕ and the longitudinal speed of the band V_L

$$V_T = \phi V_L \tag{2.1}$$

For a fixed longitudinal speed, the tracking speed is proportional to the entry angle.

4. There is assumed to be no slip between the wheel and the band. Therefore, the side-to-side position and slope of the band at the wheel entry are maintained or stored by the wheel as it rotates. These appear at the wheel exit after a half turn. Thus, the band position and slope around the wheel contain the history of the band movement during the previous half turn. As the wheel rotates, points on the band move to the wheel exit in succession as new points are added at the wheel entry.

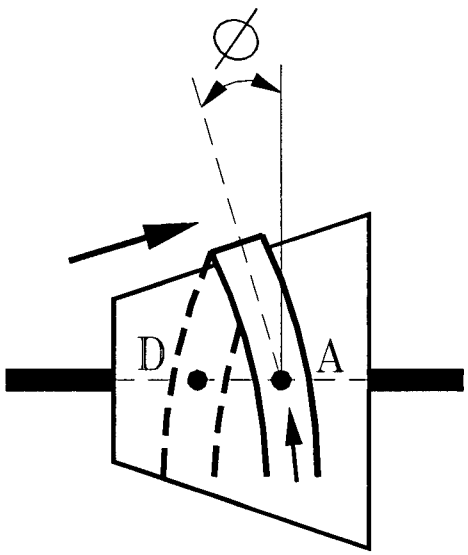

Figure 2.3: Tapered Wheel Band Shape

Figure 2.2 shows the position, shape and tracking of only a portion of a band. The position and shape of the remainder of the band can be developed by continuing the rotation of the

band shown in figure 2.2. The result is the band shown in figure 2.3. Point A is at the entry and point D is at the exit (at the far side of the wheel). The horizontal distance between points A and D corresponds to the distance tracked by the band during the previous half turn. The slope of the band at D (the exit angle) is the same as the slope at A (the entry angle). They appear to have opposite signs because opposite sides of the band are shown at points A and D.

Next consider a band running on two tapered wheels. The curved shape shown in figure 2.3 is repeated on both wheels. Since the band is continuous, the result is the figure-eight pattern shown in figure 2.4. The tracking of this band on two wheels follows the same four basic concepts presented earlier.

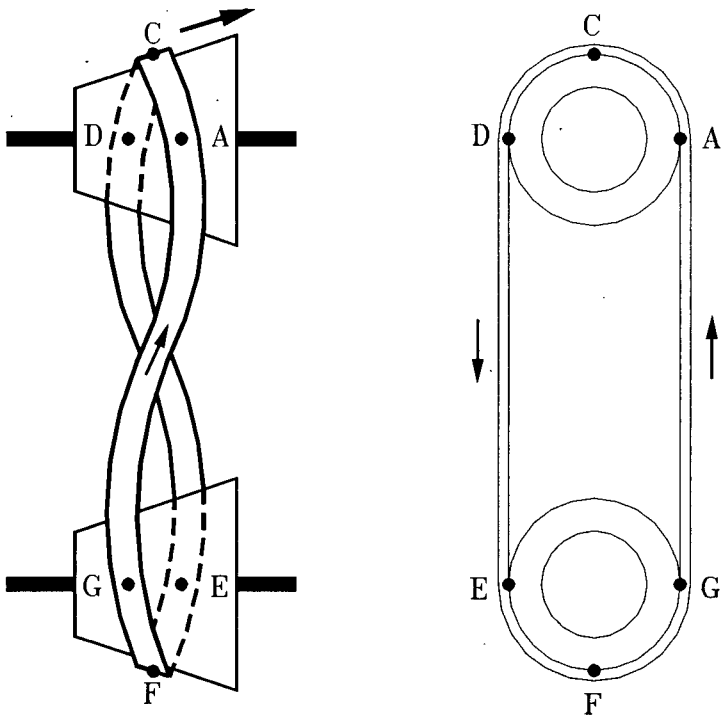

Figure 2.4: Figure-eight Pattern

Simultaneous Tracking Movement Around Two Wheels

To illustrate the simultaneous tracking movement of the band around its entire circumference, again consider the band shown in figure 2.4. The band can be divided into four sections. Two spans which are on the wheels and two free spans which are between the wheels as shown in figure 2.5. As described previously, each wheel stores the positions and slopes of the band section in contact with it, and progressively moves them to the exit point as the wheel turns. In contrast, the free spans of the band between the wheels only transmit the position and slope of the band from the exit point of one wheel to the entry point of the opposite wheel. This is done by the in-plane bending stiffness of the two free spans of the band.

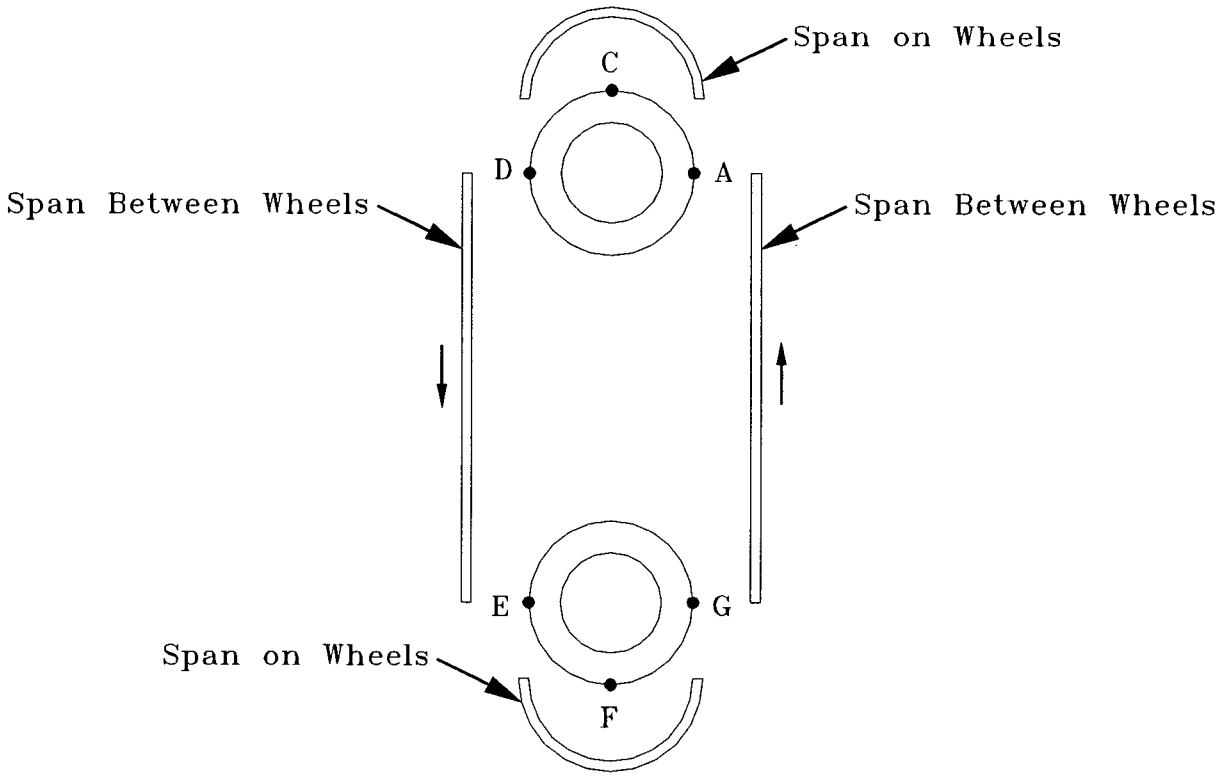

Figure 2.5: Four Sections of Band

Consider the band mounted on two tapered wheels shown in figure 2.6. The arrows numbered 1 to 10 mark the positions and slopes of the band that are in contact with the wheels. As the band and wheels rotate, the position and slope at the wheel entry points, A and E, evolve as shown in figure 2.2. Simultaneously, the stored band positions and slopes on the wheels move towards the exit points as shown in figure 2.6. The values at 1 move to 2, the values at 2 move to 3 and so on. Also at the same time, points 4 and 9 move to the wheel exit points , D and G, and their effects are transmitted by the band between the wheels to the entry points on the opposite wheels. These then affect the entry position and slope of the band during the next rotation.

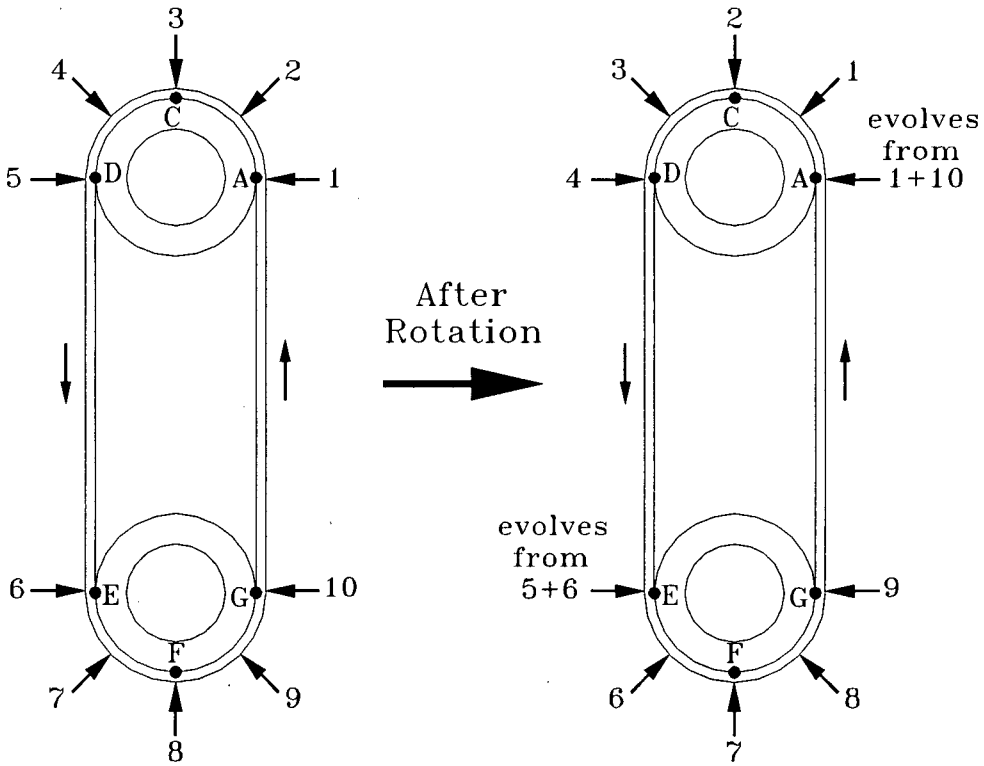

Figure 2.6: Transient Tracking Around Entire Band

2.2 Transient and Steady State Tracking

Transient and steady state tracking describe different phases of the tracking process. During transient tracking the entry angle and tracking speed of the band vary with time. However, after a number of band rotations the entry angle and tracking speed converge asymptotically to steady state values. This is steady state tracking. Later it will be shown that on a crowned wheel the steady state entry angle and tracking speed are zero. As a result, the band maintains a stable tracking position on the wheel. On a tapered wheel, the steady state entry angle and tracking speed are non-zero. As a result, the band tracks across the wheels at a constant non-zero speed.

To illustrate the mechanism of transient tracking, consider the straight band running on two flat wheels shown in figure 2.7. It was shown in figure 2.1 that in this simple case the band

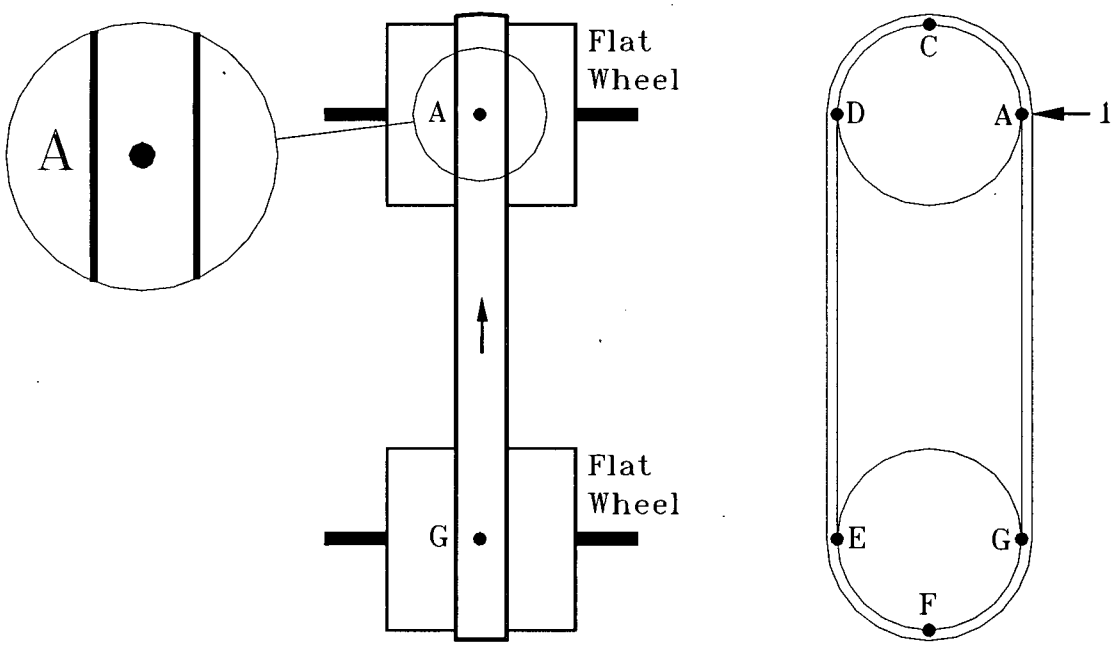

Figure 2.7: Straight Band on Two Flat Wheels

maintains a stable tracking position on the wheels as it rotates. At the instant when the band begins cutting, a feed force pushes on the center of the band between the wheels as shown in figure 2.8. Since there is no slip, the bending moment and curvature in the band created by the feed force is limited to the portion of the band between the wheels. There is no immediate effect beyond points A and G in figure 2.8. As the band rotates a small increment Δx, the band curvature changes the entry angle as shown in figure 2.9. Again due to the no slip assumption, the band slope changes only occur over the length Δx at the entry of the top wheel. At the bottom wheel exit point G, the position and slope of the band previously Δx upstream move to the exit point as explained in section 2.1. During the next rotation Δx, the non-zero entry angle creates tracking in the direction of the feed force and again the band curvature changes the entry angle as shown in figure 2.10. Again, the side-to-side position

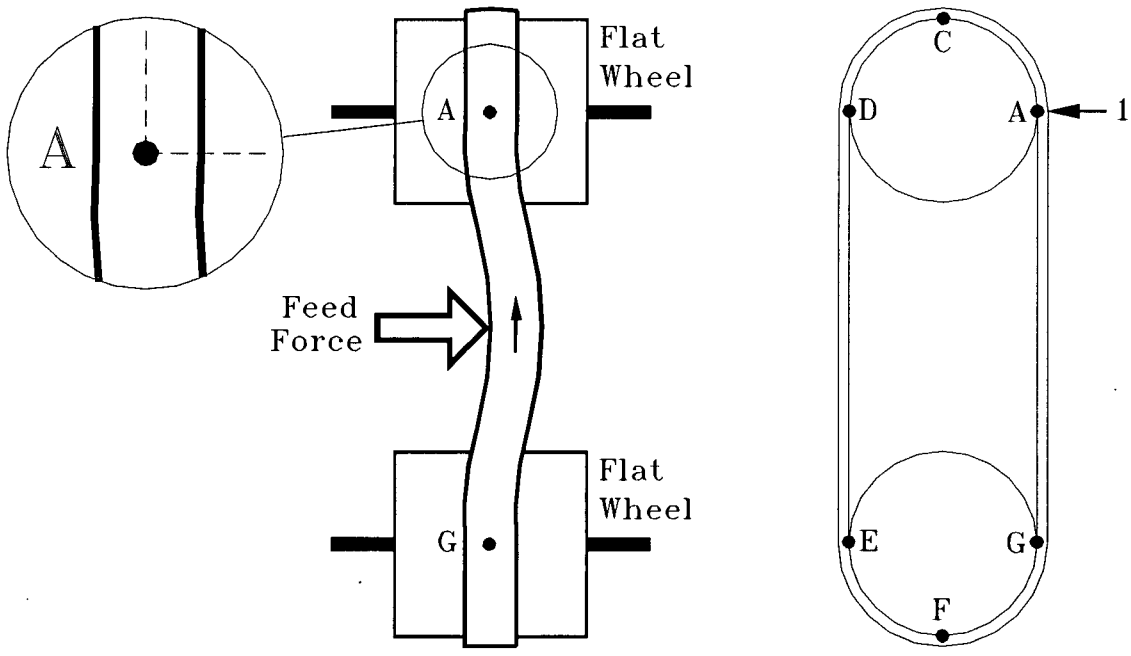

Figure 2.8: Cutting Force on Straight Band

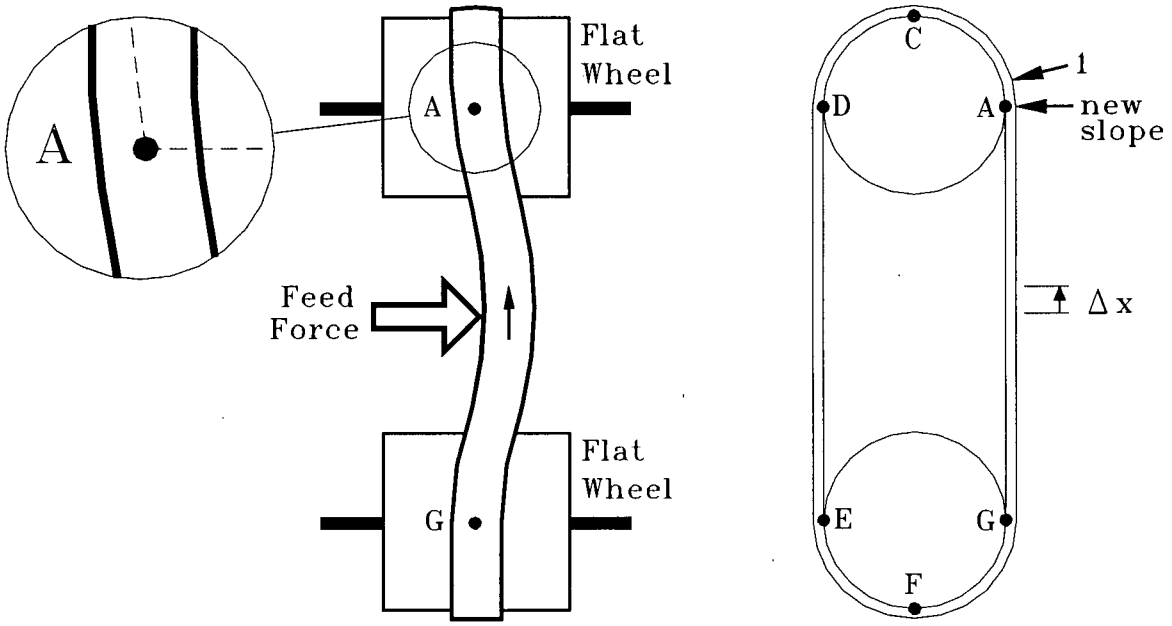

Figure 2.9: Geometry After Rotation by Δx

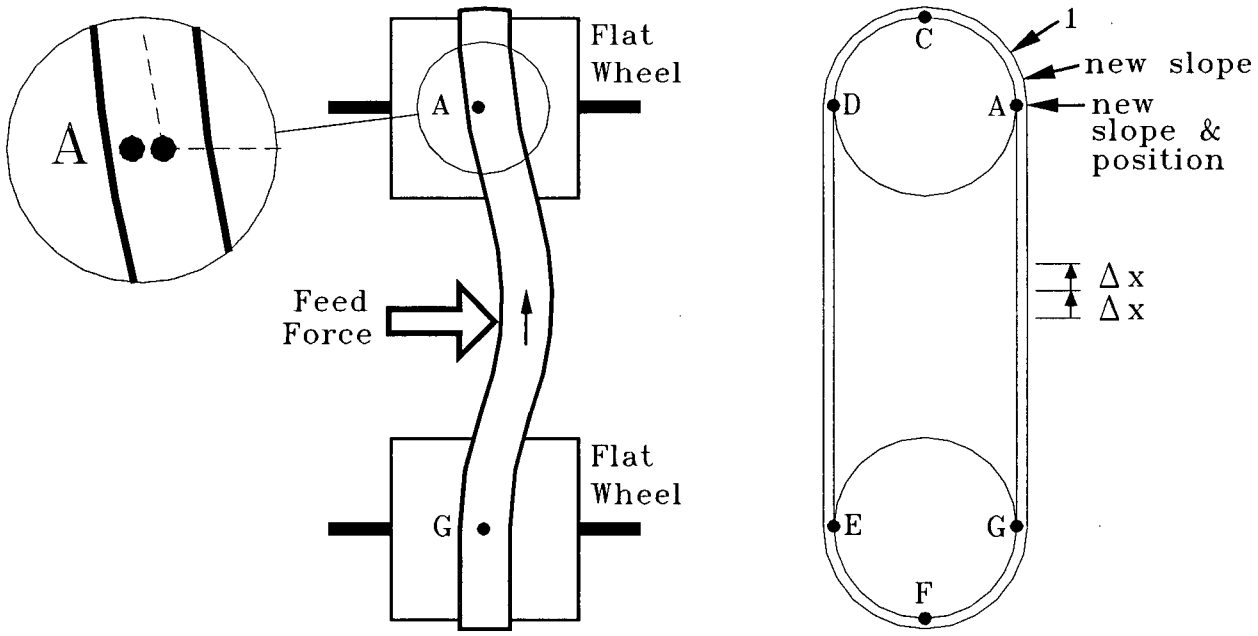

Figure 2.10: Geometry After Second Rotation by Δx

and slope of the band at the exit of the bottom wheel become those values previously Δx upstream. As a result, during transient tracking the evolution of the entry angle due to the band curvature causes the tracking speed and position to change continually.

The sequence of band tracking shown in figures 2.6, 2.7, 2.8, 2.9 and 2.10 shows that there is a delay of half a turn of the top wheel and half a turn of the bottom wheel before the feed force effect travels all the way around the band and further influences the entry angle. Figure 2.11 shows a summary of the transient tracking process.

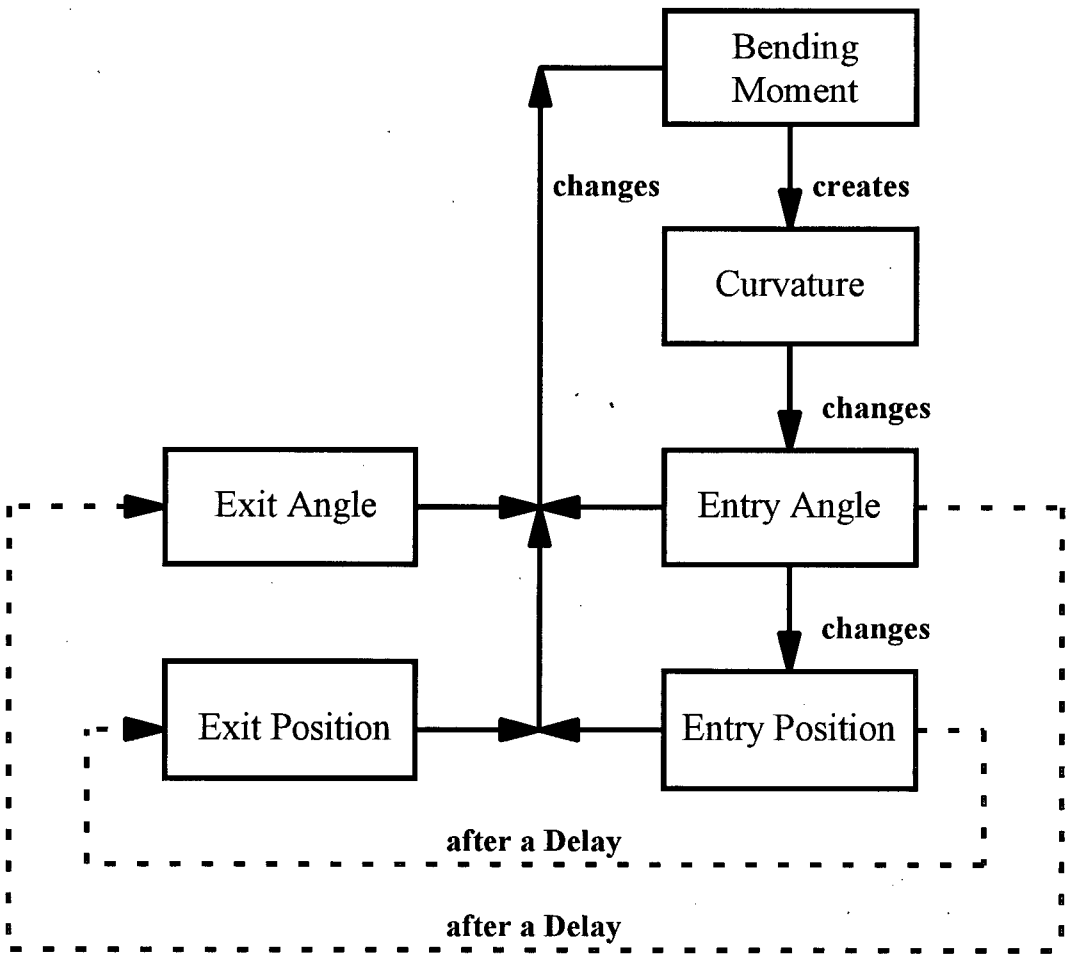

Figure 2.11: Flow Chart of Transient Tracking Process at the Entry Point

After a number of complete band rotations the entry angle and tracking speed asymptotically converge to steady state values. This is steady state tracking. It appears from figure 2.11 that steady state tracking requires the bending moment and curvature in the band to be zero. This is true when a band is tracking on flat wheels. However, consider the band which is steady state tracking on tapered wheels shown in Figure 2.12. An examination of the band at the entry point A shows that both the curvature and entry angle are non-zero. However, unwrapping the surface of the tapered wheel, as shown in figure 2.12, shows that the curvature of the wheel matches the curvature of the band at the entry point A. Therefore, steady state tracking occurs when the bending moment in the band creates a curvature which matches that of the wheel. As a result, the entry angle and tracking speed do not vary with time. Now reconsider the band tracking on flat wheels shown in figure 2.7. The flat wheel has zero curvature when unwrapped. As a result, steady state tracking occurs on flat wheels when the band curvature at the entry point is zero.

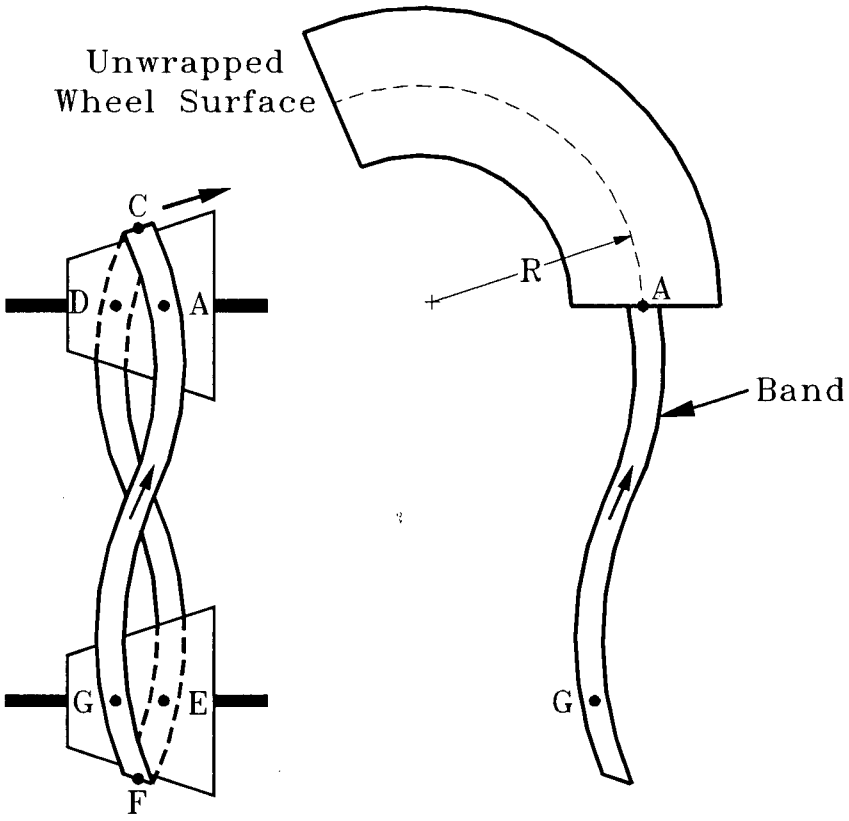

Figure 2.12: Unwrapped Tapered Wheel

3.0 Bandsaw Tracking Factors and Stability

Bandsaw tracking is the mechanism by which a saw can move sideways on the bandmill wheels during machine operation. Stable tracking occurs when the band has the tendency to return to an equilibrium position after some disturbance to its sideways motion. In practice, the most common disturbance is an in-feed (in-plane) cutting force. In section 2.3, it was shown that a in-feed cutting force creates tracking in the direction of the force. The ability of the sawblade to resist this tracking movement is a measure of its tracking stability [12,17]. A saw's tracking stability is determined by its geometry and the geometry of the bandmill wheel. In this chapter the factors that affect tracking will be examined and placed into a logical framework. The effect of these factors on the tracking stability of the bandsaw will then be examined.

3.1 Factors Affecting Tracking

The characteristics of the bandsaw blade and bandmill wheel that affect the bending moment, curvature and entry angle of the sawblade directly determine its tracking behavior. Fourteen characteristics or factors which affect tracking have been identified [6,7,8,10,12,13,14,15]. They are:

1. Wheel Profile
2. Wheel Tilt
3. Band Overhang
4. Band Strain

5. Band Width
6. Band Thickness
7. Band Tension
8. Cutting Force
9. Band Backcrown
10. Band Guides
11. Wheel Cross Line
12. Wheel and Band Coefficient of Friction
13. Band Rotational Speed
14. Band Temperature Distribution

Factors one to seven are part of a bandmill's and bandsaw's regular maintenance and set-up. Therefore, these factors will be the focus of the discussion and theoretical analysis in the next sections. The eighth factor, cutting force, will also be included in the analysis because it provides a measure of a saw's tracking stability. For simplification, only the cutting force component parallel to workpiece feed direction will be examined. Although the ninth and tenth factors, band backcrown and saw guides, are also maintenance and set-up factors, for simplification they will be excluded here. Simplifying assumptions will also be made for the final four tracking factors in the development of the theoretical model in the next section.

Wheel Profile

The tracking effect of wheel taper was illustrated earlier in figure 2.2. The wheel taper generates uneven stresses in the band, which create a bending moment, curvature and entry angle in the band. As a result, the band tracks from the small diameter up the taper to the large diameter [8].

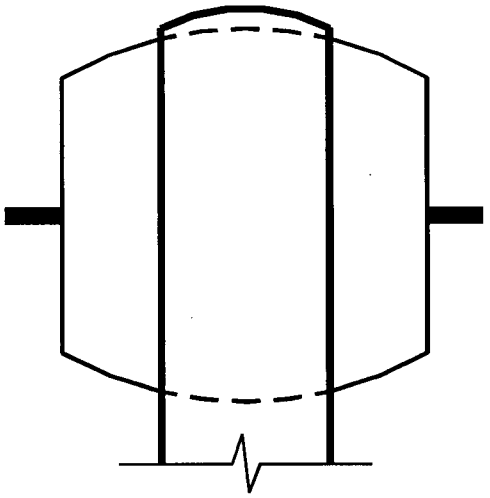

Figure 3.1: Crowned Wheel

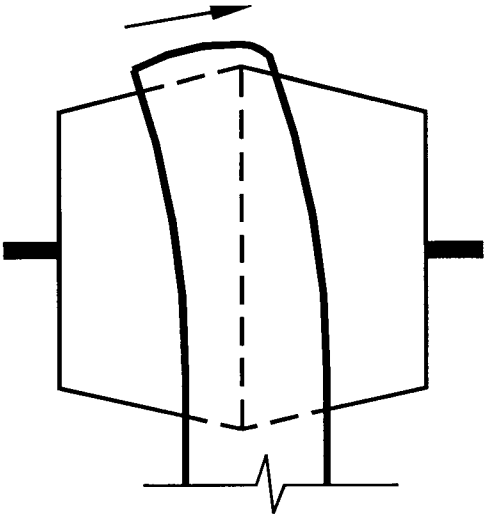

Figure 3.2: Double Tapered Wheel

In practice, bandmill wheels are rarely tapered. Typically the wheel profile consists of a smooth curved (crowned) shape similar to the one shown in figure 3.1. The tracking behavior of a band on a crowned wheel can be understood by considering the composite wheel shown in figure 3.2, consisting of two opposite tapers joined at the center. These two tapers produce tracking in opposite directions. Consider the band tracking off-center on the double tapered wheel, as shown in figure 3.2. At any time, the band can track in only one direction. Since the larger proportion of the band is running on the left taper, this side has more influence on the bending moment, curvature and entry angle. The band therefore tracks towards the wider side of the left taper, that is, towards the center of the wheel. As the band approaches the center of the wheel, the influences of the left and right tapers begin to equalize. When the band is centered on the wheel the tracking effect of the two tapers cancel and the band reaches an equilibrium position. Similarly, a band initially running more on the right taper moves

towards the wider side of the right taper, that is, towards the center of the wheel. Therefore, a band running on a crowned wheel has a natural tendency to remain at the top of the crown. This is referred to as "self centering". The bending moments and curvatures which create the self-centering effect increase with the distance that the band is displaced from the center of the crown. As a result, the self centering effect also increases with the distance between the band and the crown center.

Wheel Tilt

Wheel tilt creates an uneven stress distribution, bending moment and curvature across the band as shown in figure 3.3 [6]. The slope of the band at the entry to the top wheel creates the impression that the band will track towards the left. However, a closer examination of the

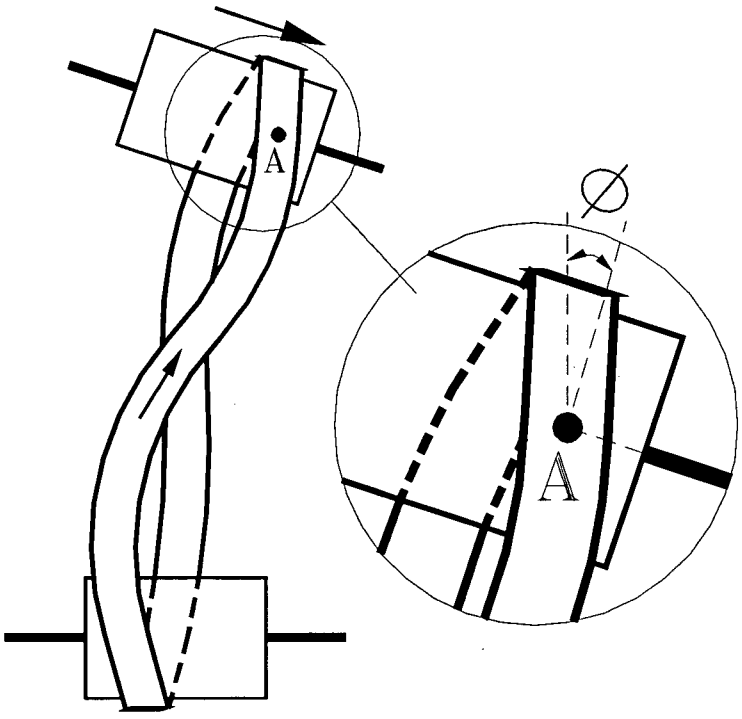

Figure 3.3: Tracking Effect of Wheel Tilt

band at the wheel entry shows that the angle of the band axis is less than the angle of wheel tilt [11]. Since the entry angle is measured relative to the wheel axis, its orientation is similar to that shown for the tapered wheel in figure 2.2. As a result, the band will track towards the right or from the higher portion down towards the lower portion of the wheel axis [6,7,8,12,13].

Band Overhang

Figure 3.4 shows a band overhanging a flat wheel. The portion of the band overhanging the wheel curls down towards the wheel as shown in figure 3.5 [6,11,18]. The curling action simulates the effect of a wheel taper, creating an uneven stress distribution, a bending moment and a curvature. As a result, the band tracks back onto the wheel. The curling action and the curvature of the band increases with overhang. As a result, the tracking effect also increases with overhang.

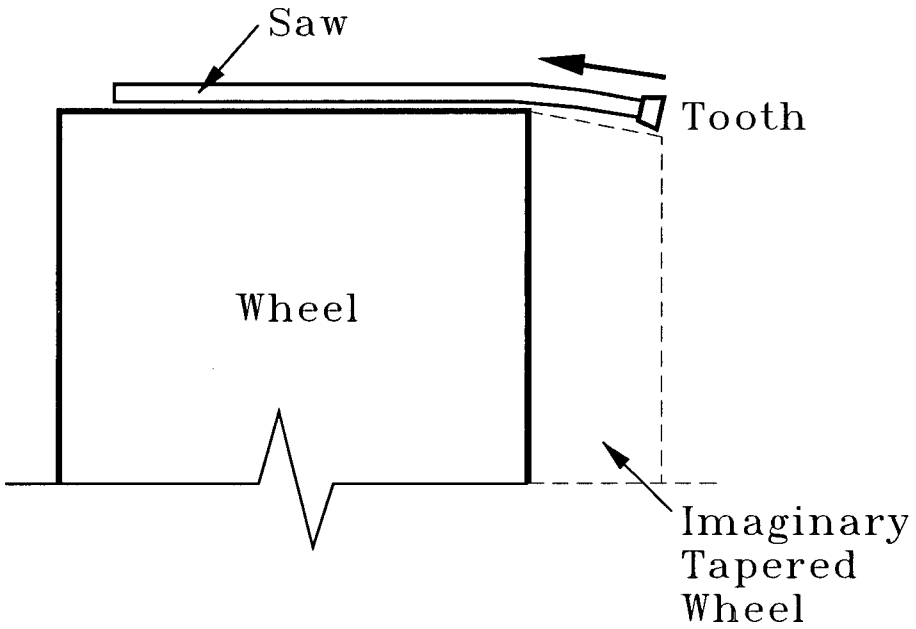

Figure 3.4: Tracking Effect of Overhang

Figure 3.5 shows a band that is overhanging both sides of the wheel. The overhang on the left side of the wheel generates a tracking effect in the opposite direction from the overhang on the right. This behavior is the same as that of the double tapered wheel shown in figure 3.1. When the overhang on the left side of the wheel is larger than that on the right, the left overhang has a larger influence on the band's bending moment, curvature and entry angle. The band, therefore, tracks to the right, that is, towards the center of the wheel. Similarly, when the overhang on the right is larger than that on the left, the band tracks towards the left, that is, towards the center of the wheel. When the band is centered on the wheel and the left and right overhangs are equal, the tracking effects cancel and the band reaches an equilibrium position. Therefore, like wheel crown, overhang has a self-centering effect that increases with the distance between the band and the wheel center.

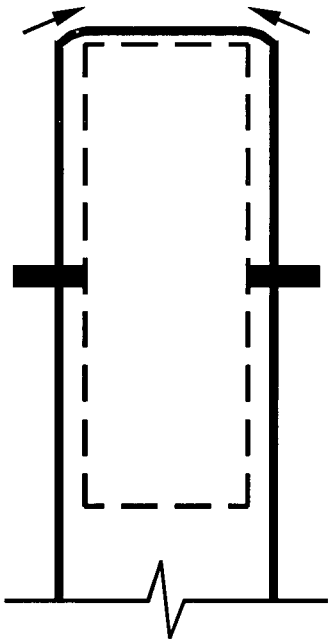

Figure 3.5: Band Overhanging Both Sides of the Wheel

Cutting Forces

The tracking effect of the in-feed cutting force was shown earlier in figures 2.8, 2.9 and 2.10. The cutting force creates a bending moment and curvature in the band. As a result, a entry angle develops between the axis of the band and the axis of the wheel and the band tracks in the direction of the cutting force.

Band Strain

Band strain by itself does not cause tracking. However, it does modify the tracking behavior caused by other factors. In the case of taper and cutting force, strain acts to straighten the band. This reduces the entry angle and correspondingly reduces the tracking speed. However, in the case of tilt, the straightening increases the entry angle and increases tracking speed. This is shown in figure 3.6. When tracking is caused by overhang, strain increases

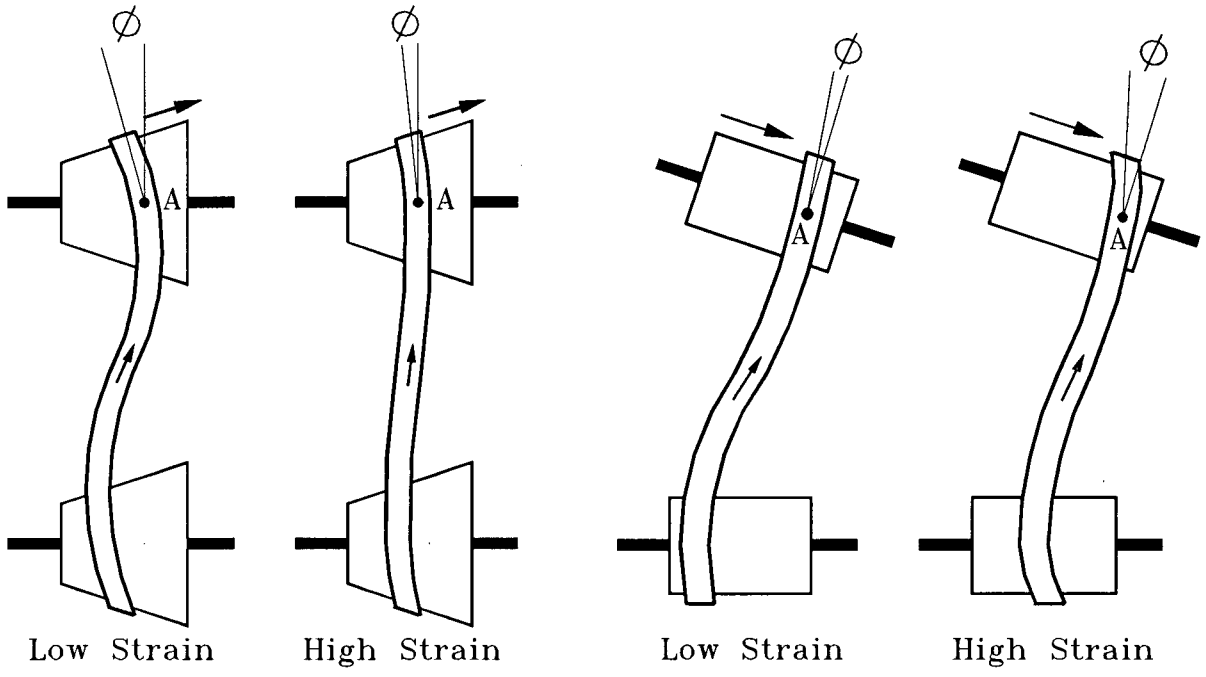

Figure 3.6: Tracking Effect of Strain

the downward curling of the overhang and as a result, also increases the bending moment that it generates. This increases the tracking effect of overhang [15].

Band Thickness and Band Width

Band thickness and width are like band strain in that they also do not individually cause tracking. However, they do affect the tracking induced by other causes. Thicker or wider bands have a higher second moment of area and therefore a higher bending stiffness. As a result, when the tracking effect is due to wheel taper, the entry angle and tracking rate are increased. However, when the tracking effect is due to a cutting force, overhang or wheel tilt, the entry angle and tracking rate are reduced.

Band Tensioning

Tensioning is a routine process used to stretch the center of a bandsaw blade by hammering or rolling its surface [3]. This process changes the shape of the saw across its width when it is wrapped around the wheel.

Band tension by itself also does not cause tracking. However, it does affect the way in which the band contacts the surface of a crowned wheel as well as the shape of the overhanging portion of the sawblade [11]. Figure 3.7 shows that tensioning can give a band a lateral profile that matches the shape of the wheel crown. This profile allows the edges of the band to contact the wheel, thereby maximizing the tracking behavior of the band. Kirbach [19]

found that flat wheels required the lowest saw tensioning and that the optimum amount of tensioning for crowned wheels increased with increasing crown height.

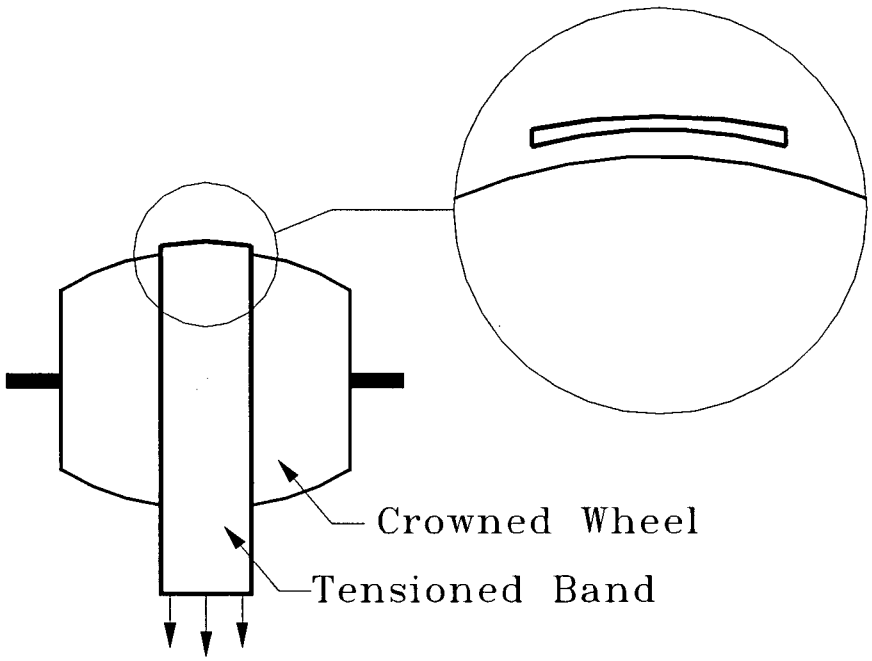

Figure 3.7: Curvature Due to Tensioning

When the sawblade overhangs the wheel, tensioning increases the downward curling of the overhanging edge. This is shown in figure 3.8. The steeper edge has the same effect as a steeper taper. Therefore, tensioning increases the tracking effect of overhang which pushes the sawblade back onto the wheel.

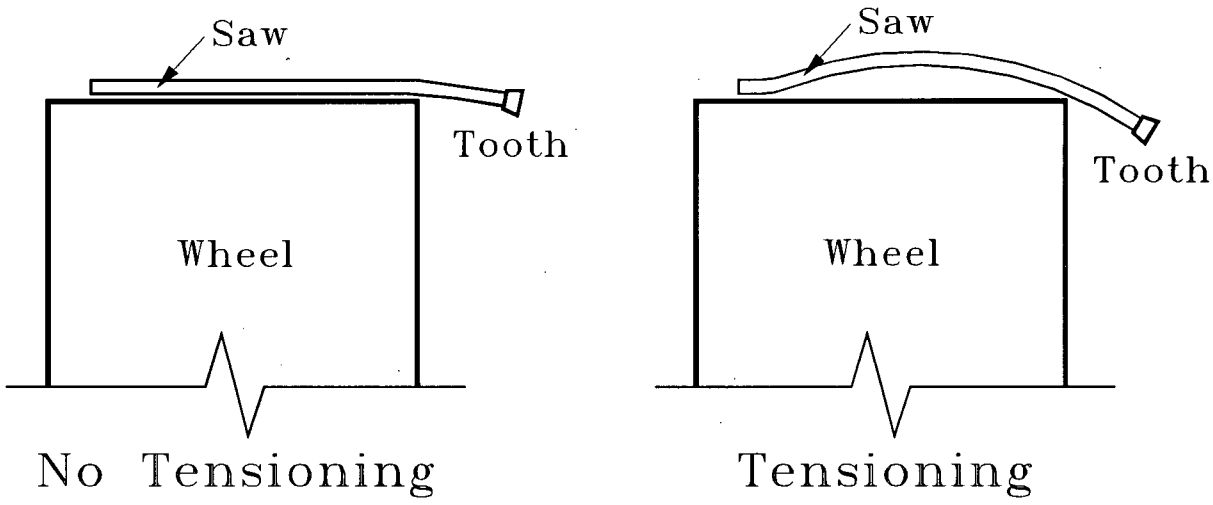

Figure 3.8: Effect of Tensioning on Overhang

3.2 Bandsaw Tracking Stability

The tracking stability of a bandsaw can be observed during sawing. Typically, when a saw is idling between cuts, it maintains a stable side-to-side position on the wheels. When the saw begins cutting, the cutting force creates a bending moment that causes the saw to track in the direction of the cutting force, as described in section 2.2. As the saw tracks from its initial position, the tracking factors generate an opposing bending moment. When the moments balance, the saw maintains a new stable position on the wheels. When the cutting force is removed the saw returns to its original position. This process of moving and generating a bending moment in response to a cutting force and then returning to the original position after the force is removed is a measure of tracking stability. A saw with a high stability is characterized as one which moves very little in response to a cutting force.

Out of the fourteen tracking factors, only wheel profile, specifically wheel crown, and overhang are true stability factors. The self centering effects of wheel crown and overhang give them the ability to:

1. Maintain the band at a stable tracking position on the wheels between cuts.
2. Generate a tracking effect in the opposite direction of the cutting force that increases as the band moves from the wheel center. When the tracking effects equalize, the band maintains a new equilibrium position.
3. Return the band to its original position after the cutting force is removed.

To illustrate the tracking stability of wheel crown and overhang consider the two straight bands shown in figure 3.9. Band A is running on crowned wheels and band B is running on flat wheels. The bands track at the center of the wheels because of the self centering effects of wheel crown on band A and overhang on band B. When the bands begin cutting, the feed forces create bending moments and curvatures in the bands. Through the process of transient tracking, bands A and B both track across the wheel in the direction of the cutting force. As bands A and B move off the centers of the wheels, the bending moments and curvatures created by the wheel crown and overhang begin to balance those created by the feed forces. Thus, bands A and B both slow down and stop at the location where the moments and curvatures balance as shown in figure 3.10. When the bands finish cutting and the feed forces are removed, the self centering effects of the wheel crown and overhang cause bands A and B to return to their original stable positions.

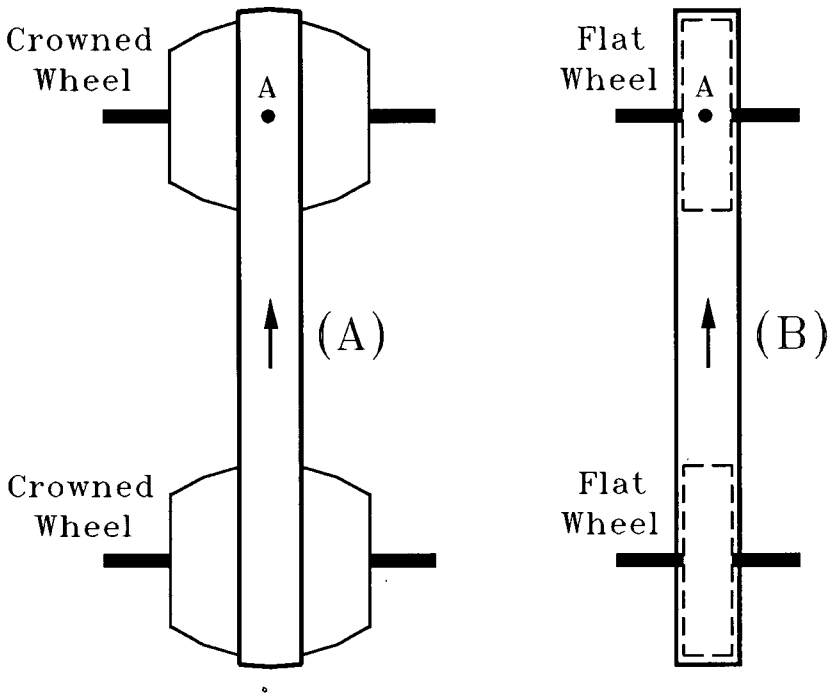

Figure 3.9: Stability of Wheel Crown and Overhang

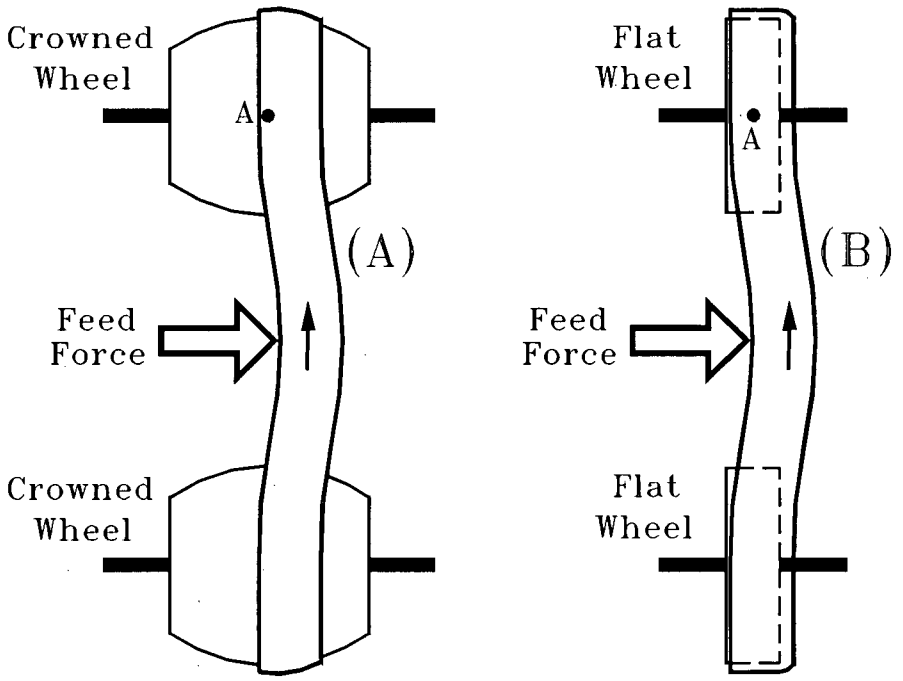

Figure 3.10: Wheel Crown & Overhang Balancing Cutting Force

The other factors such as wheel tilt, strain, width, thickness and tensioning only modify the tracking stability of wheel crown and overhang. Wheel tilt generates a constant non-zero bending moment, entry angle and tracking speed. Since this moment does not vary with tracking displacement, tilt by itself is unable to maintain the saw at a stable position on the wheels. However, when combined with wheel crown or overhang, the bending moment created by tilt does change the stable saw position on the wheels. For example, consider the band overhanging both sides of the wheel shown in figure 3.5. When the top wheel is tilted, the band tracks to the right down towards the lower portion of the axis, increasing the right overhang. When the tracking effect of the right overhang balances that of the wheel tilt, the band maintains a new stable position, as shown in figure 3.11. This becomes the new stable "center" position for the band. The remaining tracking factors, strain, width, thickness and tensioning only indirectly influence tracking stability because they are unable to generate bending moments in the band by themselves. These factors can not resist the effect of variable cutting forces if present alone.

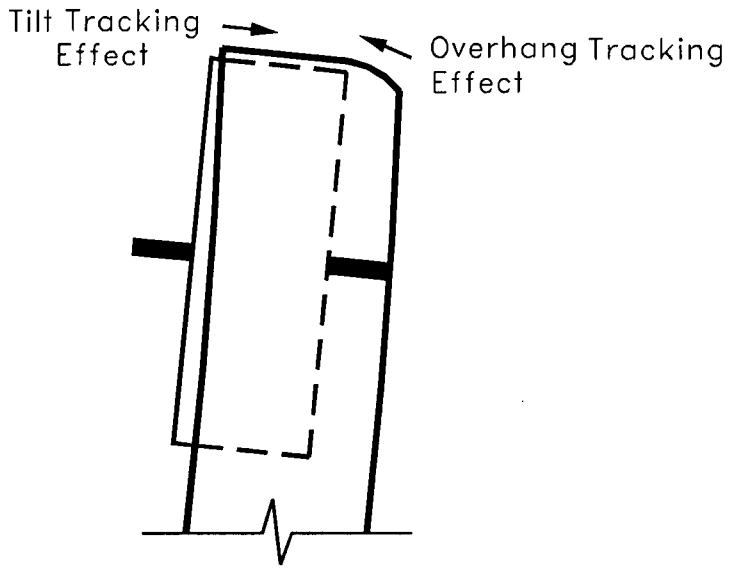

Figure 3.11: Effect of Wheel Tilt on Overhang

4.0 Theoretical Model

A theoretical model of bandsaw tracking is developed in this chapter. This model will help quantify how the tracking factors affect tracking stability. Since bandsaw tracking is affected by fourteen factors, it is possible to obtain stable tracking in many different ways. It should be possible to choose a combination of factors that produce superior tracking stability but at the same time requires less time to implement and maintain. For example, reducing the needed tensioning is a desirable goal because it is a time consuming maintenance process. Reduced tensioning has the added advantage that it makes leveling easier. The objective of the theoretical model developed in this chapter is to understand the mechanism of band tracking and to improve bandsaw tracking stability. This should allow improvements in cutting accuracy and a reduction in wheel wear and saw maintenance time.

Development of the theoretical model requires five steps. They are:

1. Make simplifying assumptions for the set-up, geometry and mechanics of the sawblade.
2. Determined the initial position and slope of the saw.
3. Develop a model of the tracking effects of the basic tracking factors. The basic factors are the wheel taper and band strain, width and thickness. The model for these factors as well as the other factors will be based on their bending moment, curvature and slope effects on the bandsaw.

4. Model the tracking of the saw as it rotates on the wheels. This will be done by using the initial position, slope and curvature of the saw and a numerical integration method to update these values as the band rotates.
5. Extend the basic model to include the effects of wheel tilt, wheel crown, cutting force, and band overhang.

4.1 Assumptions

The theoretical model will be developed with the following simplifying assumptions:

- There is no cross line between the axes of the bandmill wheels. That is, the axes lie in the same plane. This is the typical set-up for a bandmill [2].
- There are no saw guides.
- The saw has no backcrown.
- The bandsaw teeth do not significantly affect tracking and may be omitted. As a result, the saw may be considered as a uniform band.
- The coefficient of friction between the wheel and band is large enough to prevent slipping.
- The band rotational speed is slow enough that the dynamic effects are negligible.
- The temperature distribution across the band is uniform.
- The tensioning in the band allows it to contact the wheel across its entire width.
- The portion of the band between the wheels behaves as an Euler beam under axial tension [6,8].

- The portion of the band overhanging the wheels behaves like a cylindrical shell [6,11].
- The resultant of the cutting force acts in the workpiece feed direction.
- The initial position and slope of the band around the wheels can be determined reliably.

4.2 Wheel Taper and Band Strain, Thickness and Width

The simplest model of band tracking involves just four of the fourteen factors. They are wheel taper, band strain, thickness and width. This tracking model describes the side-to-side position, slope and curvature of the band at any instant in time. The model requires the initial position and slope of the band, a method of calculating the effect of the tracking factors and a method for updating the band position, slope and curvature as the band rotates and the operating conditions change.

Initial Position

The initial position and slope of the band can be determined by measuring the shape of the band on the wheels and developing an analytical equation for the position and slope of the band between the wheels. The portion of the band between the wheels can be modeled as a beam in bending under an axial tensile load [6,8] as shown in figure 4.1. The boundary conditions that determine the shape of this beam are the measured position and slope of the band at the wheel entry and exit points, A and G.

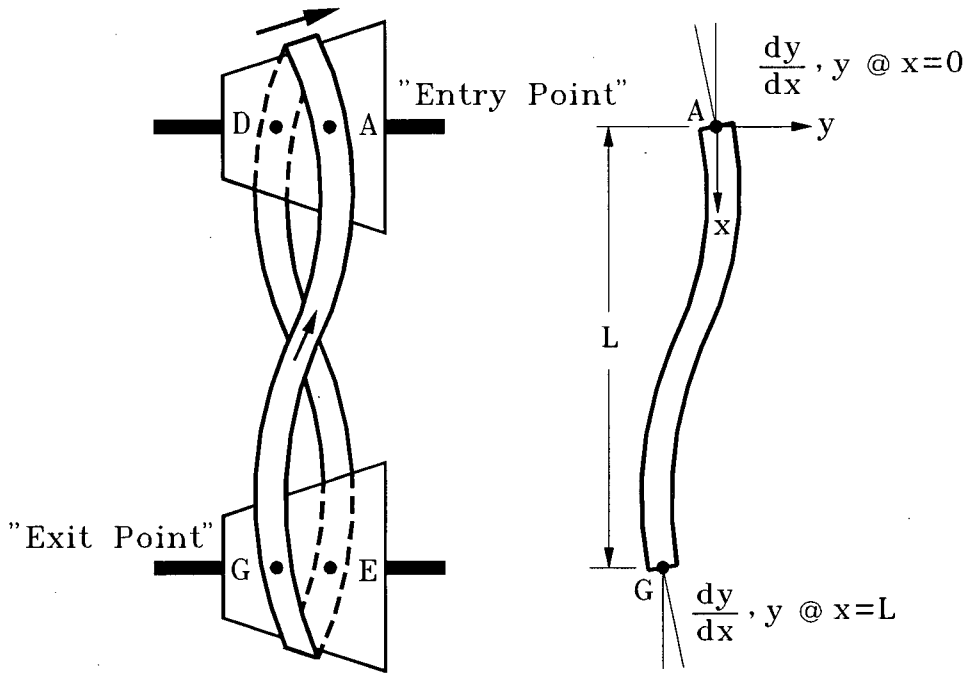

Figure 4.1: Basic Band Model

The bending moment at any point x along the length of the beam shown is figure 4.1 is

$$E I \frac{d^2y}{dx^2} = Ty + R_A x - M_A \tag{4.1}$$

where T is the axial tensile "strain" force, R_A is reaction force and M_A is the moment at point A. The general solution for equation (4.1) is [20]

$$y(x) = B_1 \sinh kx + B_2 \cosh kx + B_3 - B_4 x \tag{4.2}$$

where y is the side-to-side position of the band at a distance x from the entry point A and where

$$B_3 = \frac{M_A}{T} \tag{4.3}$$

$$B_4 = \frac{R_A}{T} \tag{4.4}$$

$$k = \sqrt{\frac{T}{E\,I}} \tag{4.5}$$

The integration constants B_1, B_2, B_3 and B_4 are calculated by applying the position and slope boundary conditions at the wheel entry and exit points. The results are:

$$B_1 = \frac{1}{k}\left[\frac{\phi_A\left(1 - \dfrac{k\,L\,\sinh(k\,L)}{\cosh(k\,L) - 1}\right) - \phi_G + y_G\,\dfrac{k\,\sinh(k\,L)}{\cosh(k\,L) - 1}}{1 - \cosh(k\,L) + \dfrac{\sinh(k\,L)\,(\,\sinh(k\,L) - k\,L\,)}{\cosh(k\,L) - 1}}\right] \tag{4.6}$$

$$B_3 = \frac{1}{\cosh(k\,L) + 1}\left[B_1\,(\sinh(k\,L) - k\,L) + \phi_A\,L - y_G\right] \tag{4.7}$$

$$B_2 = -B_3 \tag{4.8}$$

$$B_4 = (B_1\,k - \phi_A) \tag{4.9}$$

where ϕ is the slope and subscripts A and G refer to the entry and exit points of the band. Therefore, by measuring the position and slope of the band around the wheels and applying the wheel entry and exit boundary conditions to equation (4.2), the initial position of the band can be determined.

Modeling the Tracking Effects

The tracking effects of band strain, thickness and width are already modeled in the beam equation (4.2) and as a result, only the tracking effect of wheel taper requires additional consideration. An analytical equation for the effect of wheel taper can be developed by examining the bending moment created in the band. The profile of a straight tapered wheel is defined by

$$f(y) = y \tan(\gamma) \tag{4.10}$$

where γ is the taper angle shown in figure 4.2 and r and y are the radial and axial coordinates of the wheel surface profile. The zero datum for y is at a convenient point on the surface of the wheel. This point can be at the center of the wheel as shown in figure 4.2 or the top of a wheel crown. At this point, r_0 is the radius of the wheel and

$$f(0) = 0 \tag{4.11}$$

As a result, the radius, r, of the tapered wheel at any point, y, is given by

$$r = r_0 + f(y) \tag{4.12}$$

A band that is wrapped around a tapered wheel and is in complete contact with it develops a curve along its length with the same radius "R" as that of the unwrapped wheel.

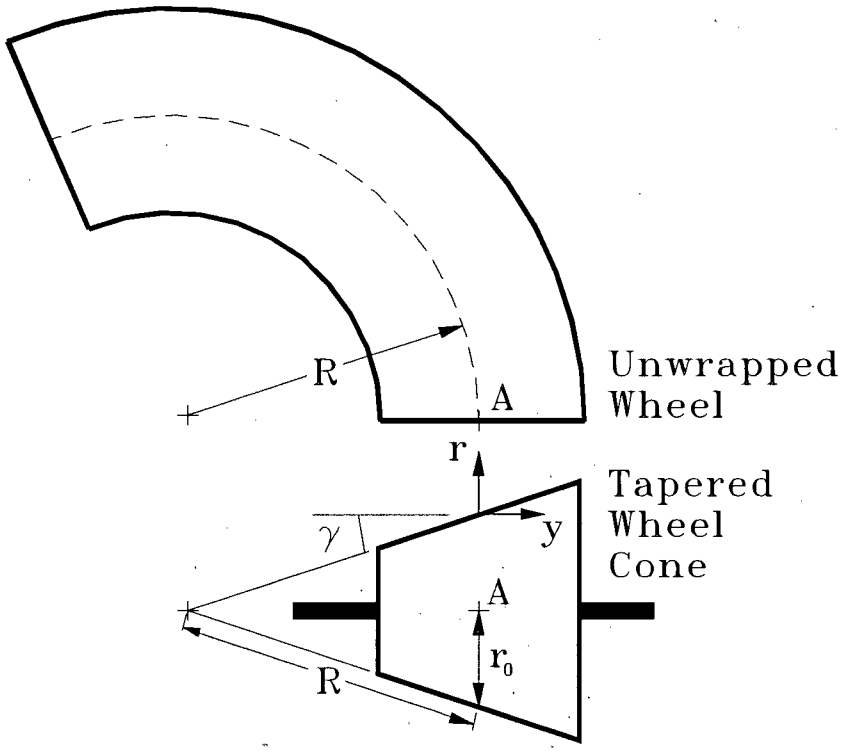

Figure 4.2: Straight Tapered Wheel

The length of the band in contact with the wheel is [8]

$$\text{contact length} = \pi\left(r_0 + f(y)\right) \tag{4.13}$$

If the original length of that section of the band, assuming no backcrown or tensioning was L_0, then the strain in the band as a result of being wrapped around the tapered wheel is

$$\varepsilon(y) = \frac{\pi\left(r_0 + f(y)\right) - L_0}{L_0} \tag{4.14}$$

and the stress in the band is given by

$$\sigma(y) = E\,\varepsilon(y) = E\,\frac{\pi\, f(y)}{L_0} + E\frac{(\pi\, r_0 - L_0)}{L_0} \tag{4.15}$$

Since the strain is small, the original length can be approximated as

$$L_0 \cong \pi\, r_0 \tag{4.16}$$

Substituting equation (4.16) into the first term of equation (4.15), the stress profile becomes

$$\sigma(y) \cong E\,\frac{\pi\, f(y)}{\pi\, r_0} + E\frac{(\pi\, r_0 - L_0)}{L_0} \tag{4.17}$$

Re-writing equation (4.17)

$$\sigma(y) = \frac{E}{r_0}\, f(y) + \sigma_0 \tag{4.18}$$

where

$$\sigma_0 = E\frac{(\pi\, r_0 - L_0)}{L_0} \tag{4.19}$$

The size of the base stress σ_0 depends mainly on the applied axial tensile "strain" force.

Equation (4.18) shows that the stress profile across the width of the band matches the profile of the wheel when the band is in complete contact with the wheel across its entire width. The

bending moment generated by the wheel profile is calculated by integrating the stress profile given by equation (4.18) across the width "b" of the band about its centerline [8,11]

$$M = \int_{-\frac{b}{2}}^{\frac{b}{2}} \sigma(y)\ h\ y\ dy \tag{4.20}$$

where h is the thickness and the datum, y = 0, is at the centerline of the band. After substituting equation (4.18), equation (4.20) becomes

$$M = \frac{E\,h}{r_0} \int_{-\frac{b}{2}}^{\frac{b}{2}} f(y)\,y\,dy \tag{4.21}$$

The second constant term in equation (4.18) has no contribution to the moment M because of symmetry.

$$\int_{-\frac{b}{2}}^{\frac{b}{2}} \sigma_0\ dy = 0 \tag{4.22}$$

Therefore, the tracking effect of wheel taper is determined by substituting the wheel taper equation (4.10) into equation (4.21). Later, the bending moment given by equation (4.21) will be used in the numerical integration model of tracking to update the entry angle as the band rotates.

Modeling the Simultaneous Tracking Movement

The simultaneous tracking movement around the entire band is modeled as shown in figures 2.6 and 2.11. The measured position and slope of the band around the wheel and the calculated shape of the band between the wheels provides the initial position of the entire band. As shown in figure 2.6, when the band rotates, the position and slope the band on the wheels moves incrementally towards the wheel exit. At the same time, the values appearing at the wheel exit are transmitted to the entry point of the opposite wheel by the portion of the band between the wheels. This is modeled using equation (4.1). Therefore, the remaining step is to model the evolution of the band position and slope at the wheel entry point. This can be modeled and calculated with sufficient accuracy using the Euler numerical integration method.

The basic steps of the Euler method are shown in figure 2.11. After the band rotates a distance Δx, the band's new position at the wheel entry is calculated from the current ("old") position and slope, y_{old} and $\frac{dy}{dx}_{old}$. Since the slope is approximately

$$\frac{dy}{dx} \cong \frac{\Delta y}{\Delta x} = \frac{y_{new} - y_{old}}{\Delta x} \tag{4.23}$$

the new position is calculated by

$$y_{new} = y_{old} + \frac{dy}{dx}_{old} \Delta x \tag{4.24}$$

The new slope or entry angle of the band is calculated from the initial slope and the curvature of the band and wheel. In section 2.2, it was explained that the difference between the curvature of the band and the curvature wheel of the wheel, $\frac{1}{R}$, at the entry point acts to change the entry angle as the band rotates. Therefore, since the difference between the curvature of the band and the wheel is approximately

$$\left(\frac{d^2y}{dx^2}_{band} - \frac{1}{R}\right) \cong \frac{\Delta\left(\frac{dy}{dx}\right)}{\Delta x} = \frac{\frac{dy}{dx}_{new} - \frac{dy}{dx}_{old}}{\Delta x} \tag{4.25}$$

the new entry angle is calculated by

$$\frac{dy}{dx}_{new} = \frac{dy}{dx}_{old} + \left(\frac{d^2y}{dx^2}_{band} - \frac{1}{R}\right) \Delta x \tag{4.26}$$

The curvature of the band at the wheel entry point is calculated by differentiating equation (4.2) twice and substituting in the location of the entry point

$$\frac{d^2y}{dx^2}_{band}(0) = B_2 k^2 \tag{4.27}$$

The bending moment generated in the band by the tapered wheel is calculated from equation (4.21). Finally, the beam curvature produced by this bending moment is

$$\frac{1}{R} = \frac{d^2y}{dx^2}_{Wheel} = \frac{M}{E\,I} = \frac{h}{I\,r_0}\int_{-\frac{b}{2}}^{\frac{b}{2}} f(y)\,y\,dy \qquad (4.28)$$

Applying this numerical integration method to the band at the entry points of both wheels, updating the position and slope of the band around the wheel and calculating the shape of the band between the wheels using equation (4.2), allows the tracking of the entire band to be calculated.

In summary, the tracking process is calculated here using the following iteration scheme:

1. Determine the current position and slope of the band from the initial shape.
2. Calculate the curvature of the band at the wheel entry from equations (4.2) and (4.27).
3. The band is moved by a small amount Δx. The position and slope of the band on the wheels are moved towards the exit points. The position and slope of the band at the exits point take on the values previously existing at a point Δx upstream.
4. Calculate the new position and slope at the wheel entry from equations (4.24) and (4.26).
5. The new band position and slope in equations (4.24) and (4.26) become the old values.
6. Calculate the band shape between the wheels from equation (4.2) using the old boundary conditions at the wheel entry and exit points.

Repeated application of steps 2 to 6 models the simultaneous and continuous tracking of the band around its entire length. After a number of band rotations, the entry angle converges to a steady state value ϕ_S. This value coincides with the value determined by Swift [8]

$$\phi_S = \frac{2L}{L_T k}\left(\frac{\sinh(kL)}{\cosh(kL)-1} - \frac{2}{kL}\right)\left(\frac{2\gamma_1}{D_1} - \frac{2\gamma_2}{D_2}\right) \tag{4.29}$$

where L_T is the total length of the band and subscripts 1 and 2 refer to the top and bottom wheels respectively.

4.3 Bandmill Wheel Tilt

Wheel tilt can be added to the basic tracking model by examining its effect on the portion of the band between the wheels. Figure 2.4 shows the initial shape of a band tracking on two tapered wheels. Figure 4.3 shows the shape after the top wheel is tilted by an angle β. As explained in section 3.1, at the instant when the wheel is tilted, only the portion of the band between the wheels is affected. That is, the bending moment and curvature changes are isolated to the portion of the band between the wheels. Consequently, wheel tilt can be modeled as a change in the slope boundary condition for the portion of the band between the wheels [8]. The wheel tilt slope boundary conditions at the entry and exit points of the wheel are

$$\frac{dy}{dx}_{tilt} = \frac{dy}{dx} + \beta \tag{4.30}$$

The change in the shape and curvature of the band between the wheels is calculated by applying the new boundary conditions to equations (4.2) and (4.27). As in the basic model, after a number of band rotations, the entry angle converges to a steady state value ϕ_S. This value again coincides with the value determined by Swift [8]

$$\phi_S = \frac{2L}{L_T k}\left(\frac{\sinh(kL)}{\cosh(kL)-1}-\frac{2}{kL}\right)\left(\frac{2\gamma_1}{D_1}-\frac{2\gamma_2}{D_2}\right) - \frac{\beta L}{L_T}\left(1-\frac{2(\sinh(kL)-kL)}{kL(\cosh(kL)-1)}\right)$$

.....(4.31)

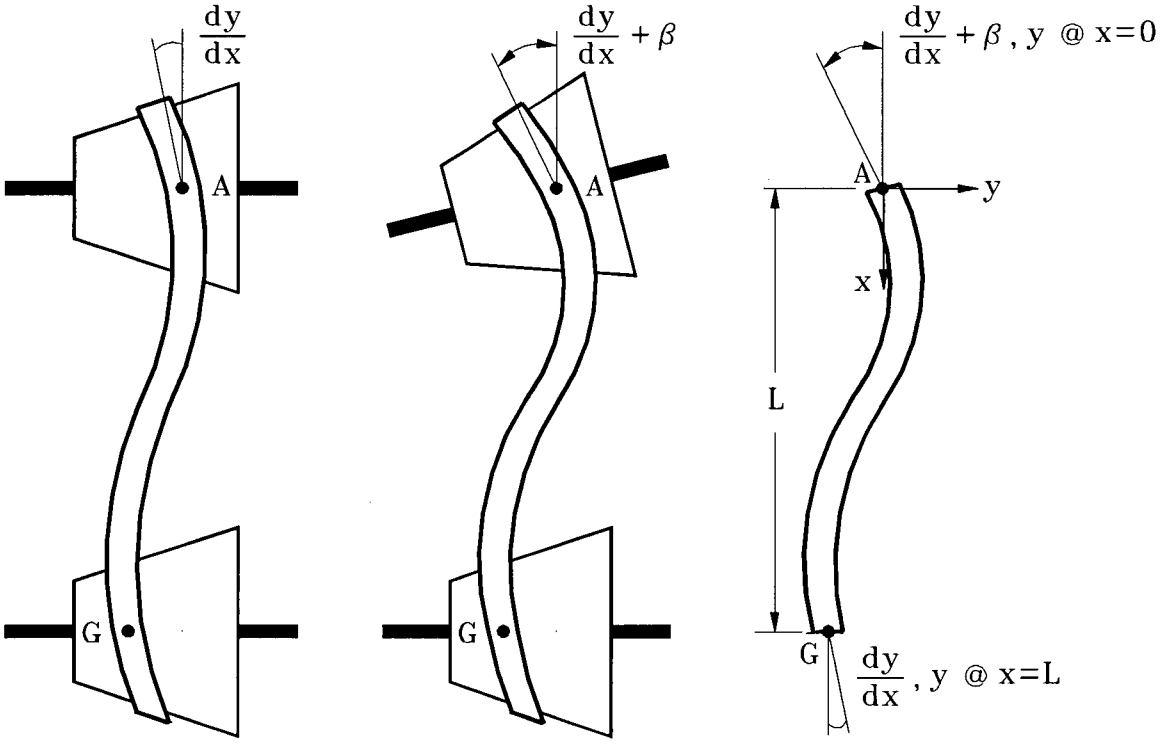

Figure 4.3: Boundary Conditions due to Wheel Tilt

4.4 Bandmill Wheel Profile

The tracking model developed in the first three sections describes the tracking of a band on tapered wheels. On tapered wheels the bending moment and curvature generated in the band by the wheel profile are constant, as shown by equations (4.21) and (4.28). On crowned wheels the bending moment and curvature generated in the band changes with the distance between the band centerline and the crown center. To extended the tracking model to include more general wheel profiles such as wheel crown, consider the crowned wheel profile described by

$$f(y) = a\,y^2 \tag{4.32}$$

where "a" is a constant that adjusts the crown height. Substituting equation (4.32) into equation (4.18) gives the stress profile across the width of the band when it is tracking on the center of the crown. When the band is tracking at a distance, u, from the center of the crown, the bending moment and curvature in the band are calculated by

$$M(u) = \frac{E\,h}{r_0} \int_{u-\frac{b}{2}}^{u+\frac{b}{2}} f(y)\,(y-u)\,dy \tag{4.33}$$

$$\frac{1}{R} = \frac{d^2y}{dx^2}(u)_{\text{Wheel}} = \frac{M(u)}{E\,I} \tag{4.34}$$

Replacing equations (4.21) and (4.28) with equations (4.33) and (4.34) extends the tracking model to include wheel profiles where the bending moment and curvature generated by the wheel profile change as the band moves across the wheel.

4.5 Bandsaw Overhang

In section 3.1 it was shown that overhang behaves like a tapered extension to a wheel. A close examination of the overhang in figure 3.4 shows that it is a smooth curve similar to a wheel crown. Therefore, overhang is modeled here as a wheel crown extension to the wheel surface. The equivalent crown shape is modeled by evaluating the profile of the overhanging part of the band. For simplicity, the slope of the wheel surface is assumed to be zero at the edge where the overhang occurs.

Sugihara [6] and Taylor [11] modeled the overhang as a cylindrical shell. One edge of the shell is free while the other edge has an applied shear force and bending moment. The shear force and bending moment were derived from the displacement of the bandmill wheel. Using a different approach, the overhang is modeled here as a cylindrical shell rigidly clamped at one edge and free at the other, as shown in figure 4.4. A uniform external pressure P is applied to the shell. This pressure corresponds to the radial force per unit area acting on the band required to maintain equilibrium with the "strain" force T around the curved surface, as shown in figure 4.5.

$$P = \frac{T}{r_0 b} \tag{4.35}$$

where b is the band width and r_0 is the mean wheel radius. Over the portion of the band in contact with the wheel, this radial force per unit area is balanced by the contact pressure between the band and wheel.

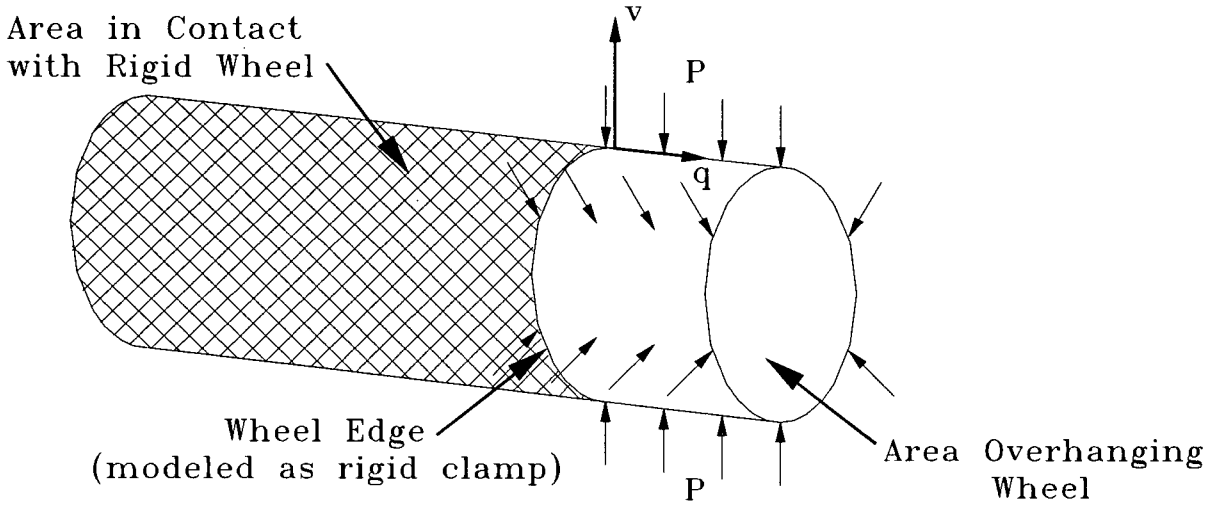

Figure 4.4: Cylindrical Shell Model of Overhang

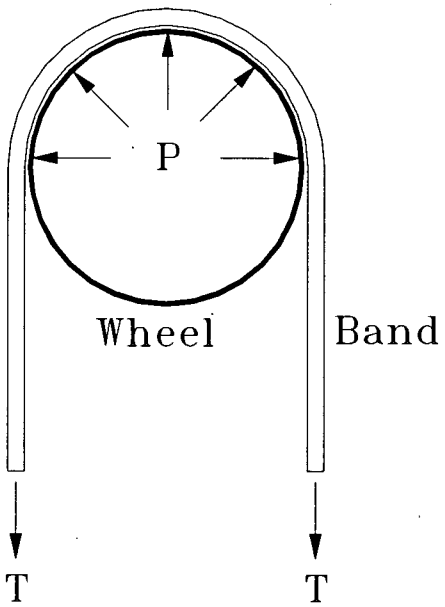

Figure 4.5: Uniform Pressure on Band

The equation for the radial deformation, w, of a circular cylindrical shell symmetrically loaded by a uniform pressure P is [22]

$$\frac{d^4w}{dq^4} + 4\eta^4 w = \frac{-P}{D} \tag{4.36}$$

where q and v are the axial radial coordinates and

$$\eta^4 = \frac{3(1-\nu^2)}{r_0^2 h^2} \tag{4.37}$$

$$D = \frac{E h^3}{12\left(1-\nu^2\right)} \tag{4.38}$$

The general solution for equation (4.36) is

$$w(q) = e^{\eta q}\left[C_1 \cos(\eta q) + C_2 \sin(\eta q)\right] + e^{-\eta q}\left[C_3 \cos(\eta q) + C_4 \sin(\eta q)\right] - \frac{P}{4\eta^4 D} \tag{4.39}$$

where C_1, C_2, C_3 and C_4 are integration constants that are determined from the boundary conditions. The deformation boundary condition for the clamped end of the shell is

$$w(0) = 0 \tag{4.40}$$

and assuming that the edge of the wheel has zero slope

$$\frac{dw}{dq}(0) = 0 \tag{4.41}$$

At the free end of the shell the boundary conditions are

$$\text{moment} \qquad M(d) = E\,I\,\frac{d^2w}{dq^2}(d) = 0 \tag{4.42}$$

$$\text{shear} \qquad V(d) = E\,I\,\frac{d^3w}{dq^3}(d) = 0 \tag{4.43}$$

where d is the overhanging length. If constants H and J are defined as

$$H = \frac{e^{\eta d}\sin(\eta d) - e^{-\eta d}\left[\,2\cos(\eta d) - \sin(\eta d)\,\right]}{\left(e^{\eta d} + e^{-\eta d}\right)\cos(\eta d)} \tag{4.44}$$

$$J = \frac{\dfrac{-P}{4\eta^4 D}\,e^{-\eta d}\left[\,\sin(\eta d) - \cos(\eta d)\,\right]}{\left(e^{\eta d} + e^{-\eta d}\right)\cos(\eta d)} \tag{4.45}$$

then the results of applying the boundary conditions are

$$C_1 = \frac{2\,\dfrac{-P}{4\eta^4 D}\,e^{-\eta d}\cos(\eta d) - J\left[e^{\eta d}\left(\cos(\eta d) - \sin(\eta d)\right) - e^{-\eta d}\left(\cos(\eta d) + \sin(\eta d)\right)\right]}{e^{\eta d}\left[\,(H-1)\cos(\eta d) - (H+1)\sin(\eta d)\,\right] - e^{-\eta d}\left[\,(H+3)\cos(\eta d) + (H+1)\sin(\eta d)\,\right]}$$

..... (4.46)

$$C_2 = H\,C_1 + J \tag{4.47}$$

$$C_3 = \left(\frac{P}{4\eta^4 D} - C_1\right) \tag{4.48}$$

$$C_4 = \frac{-P}{4\eta^4 D} - 2C_1 - C_2 \qquad (4.49)$$

Figure 4.6 shows overhang on a flat wheel. Again, r and y are radial and axial coordinates at

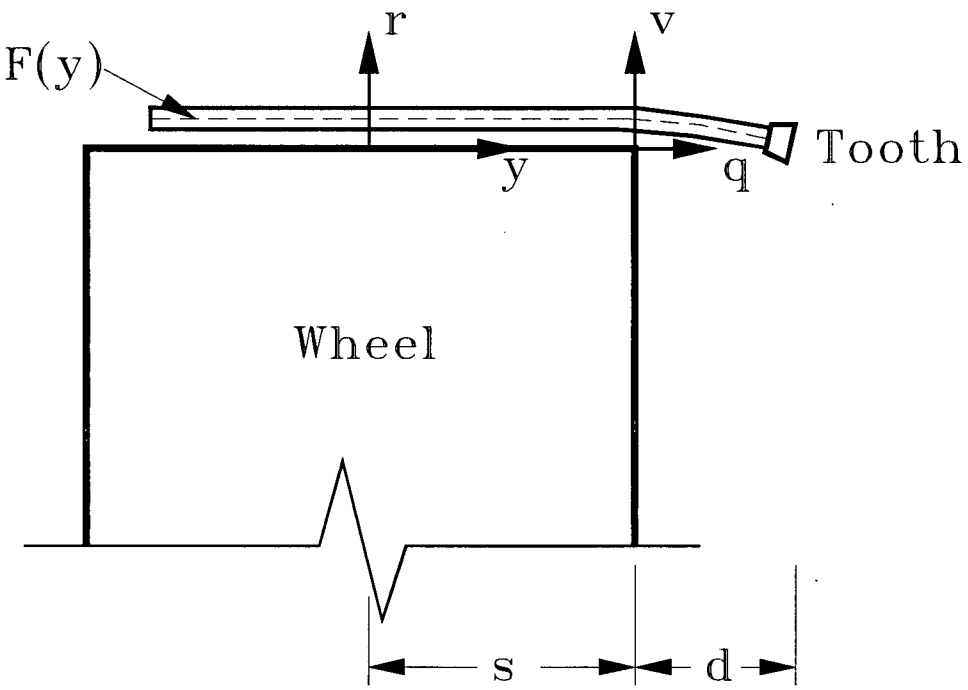

Figure 4.6: Overhang of a Flat Cylindrical Wheel

a convenient location on the surface of the wheel. "s" is the distance from y = 0 to the overhang wheel edge. The length, d, of the overhanging section is

$$d = \left\langle u + \frac{b}{2} - s \right\rangle \qquad (4.50)$$

where "u" is the distance between the band center and wheel center and the singularity function "$\langle\tau\rangle$" is defined as

$$\langle \tau \rangle = 0 \quad \text{when} \quad \tau < 0$$

and

$$\langle \tau \rangle = \tau \quad \text{when} \quad \tau \geq 0$$

Therefore, the overhang coordinate q and the overhang deformation can be written as functions of y

$$q = \langle y - s \rangle \tag{4.51}$$

$$w(q) = w\left(\langle y - s \rangle\right) \tag{4.52}$$

Since overhang behaves as an extension of the wheel profile f(y), the combined profile is given by

$$\underbrace{F(y)}_{\substack{\text{equivalent} \\ \text{wheel profile}}} = \underbrace{f(y)\,\langle s - y \rangle^0}_{\text{on wheel}} + \underbrace{w\langle y - s \rangle^0}_{\text{overhang}} \tag{4.53}$$

Since the stress profile in the band matches the wheel profile, the bending moment is calculated by

$$M(u) = \frac{E\,h}{r_0}\left[\int_{u-\frac{b}{2}}^{s} f(y)\,(y-u)\,dy + \int_{s}^{u+\frac{b}{2}} w(y-s)\,(y-u)\,dy\right] \tag{4.54}$$

when the overhang $d > 0$ or $u + \frac{b}{2} > s$. Otherwise, equation (4.33) is used. The tracking effect of overhang can be incorporated into the tracking model by calculating the curvature resulting from the bending moment using equation (4.34) and including it as the wheel curvature in equation (4.26).

4.6 Cutting Force

The cutting force can be included in the theoretical model as a concentrated force acting on the edge of the band between the wheels as shown in figure 4.7. Equation (4.2) for a beam in bending and under an axial tensile load can be extended to included a concentrated edge force F [22]. For simplicity, here the force is modeled as being at the center of the band length.

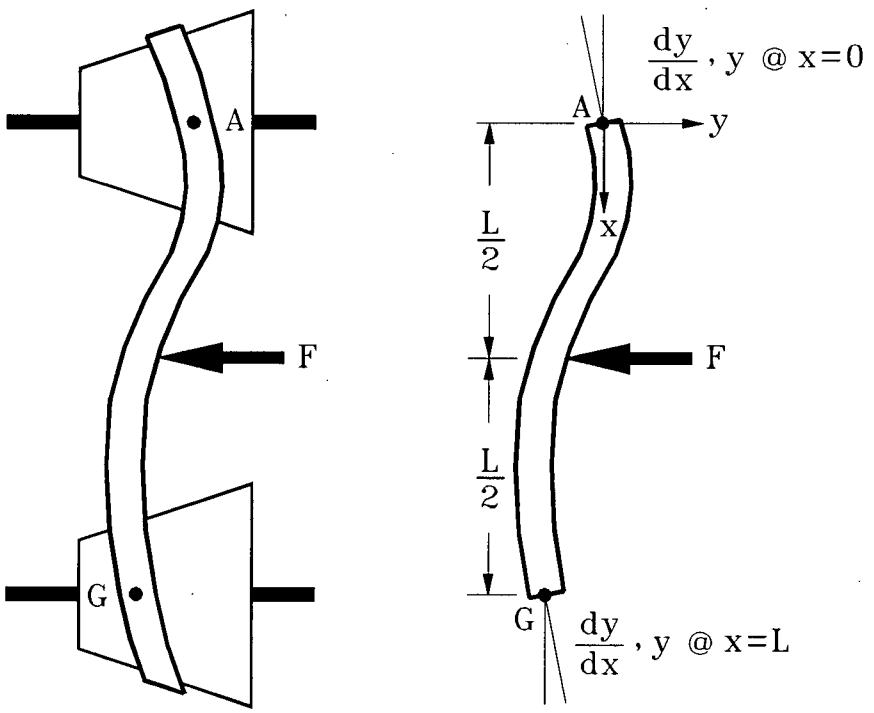

Figure 4.7: Cutting Force Model

The general beam equation (4.2) becomes [23]

$$y(x) = y_A + \frac{\theta_A}{k}\sin(kx) + \frac{M_A}{T}\left(1-\cos(kx)\right) + \frac{R_A}{kT}\left(kx - \sin(kx)\right) - \frac{F}{kT}\left(k\left\langle x - \frac{L}{2}\right\rangle - \sin k\left\langle x - \frac{L}{2}\right\rangle\right)$$

.....(4.55)

where the moment at the entry point A is

$$M_A = \frac{T}{k\sin(kL)}\left[\theta_B - \theta_A\cos(KL) - \frac{R_A}{T}\left(1-\cos(kL)\right) + \frac{F}{T}\left(1-\cos\right)\left(\frac{kL}{2}\right)\right]$$

.....(4.56)

and the reaction force at the same point is

$$R_A = \left(\frac{\left(1-\cos(kL)\right)^2}{Pk\sin(kL)} - \frac{\left(kL-\sin(kL)\right)}{Pk}\right)$$
$$\left[y_A + \theta_A\left(\frac{\sin(kL)}{k} - \frac{\cos(kL)-\cos^2(kL)}{k\sin(kL)}\right) + \theta_A\left(\frac{(1-\cos(kL)}{k\sin(kL)}\right) + F\left(\frac{\left(1-\cos(kL)\right)\left(1-\cos\left(\frac{kL}{2}\right)\right)}{Pk\sin(kL)} - \frac{L}{2T} + \frac{\sin\frac{kL}{2}}{kT}\right)\right]$$

.....(4.57)

In summary, equations (4.30), (4.32), (4.33), (4.39), (4.54) and (4.55) model the tracking effects of cutting force, wheel profile and tilt and band overhang, strain, thickness and width. Equations (4.24), (4.26) and (4.34) enable updating of the band position and slope at the wheel entry point and complete the model of band tracking.

5.0 Verifying the Theoretical Model

Several series of experiments were performed in order to explore the tracking behavior of a moving band and to validate the theoretical model of tracking. These experiments include an examination of the basic tracking model of wheel taper and band strain, thickness and width followed by an examination of the wheel tilt, wheel crown, cutting force and overhang. Band tensioning will not be examined because it is difficult to produce reliably using the available equipment.

A table-top bandmill model was designed and built to allow detailed measurements of band tracking behavior. For these exploratory measurements, a table-top model is preferred over a full-size bandmill because the various machine adjustments and tracking measurements can be made more accurately and conveniently.

5.1 Equipment

Figure 5.1 shows the table-top bandmill model. The model consists of a mounting frame, a flat wheel, a profiled wheel, a thin straight band made from brass shim stock, and a feed force applicator to simulate the cutting force. Figure 5.2 summarizes the main dimensions. The flat wheel is mounted in fixed bearings. The profiled wheel is mounted parallel to the flat wheel in two take-up bearings. The take-up bearings can be adjusted so as to move the wheels apart and apply strain to the band. The size of the strain is determined by measuring the extension

of calibrated coil springs attached to the take-up bearing housing. Finally, the cutting force applicator consists of a pulley wheel pushing against the side of the band at the midpoint of its free span between the wheels.

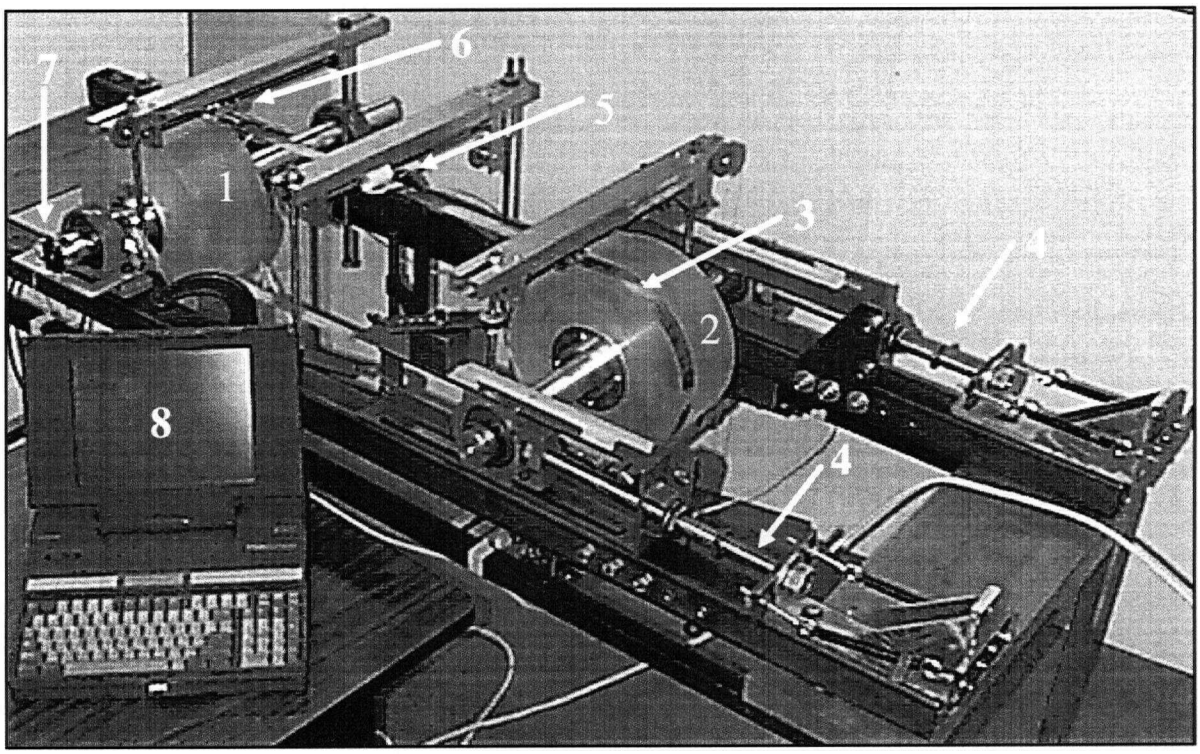

#	ITEM
1	Flat Wheel
2	Profiled Wheel
3	Metal Band
4	Strain Applicator (take-up unit and spring)
5	Cutting Force Applicator
6	Linear Optical Encoder
7	Rotary Optical Encoder
8	Computer

Figure 5.1: Table Top Model

Wheel	Diameter, in
Profiled	11.5
Flat	11.6

Band #	Width, in	Thickness, in	Length, in
1	0.50	0.002	99
2	0.64	0.002	99
3	0.75	0.002	99
4	0.93	0.002	99
5	1.13	0.002	99

Figure 5.2: Wheel and Band Dimensions

Four linear optical encoders measure the tracking position and movement of the band at the entry and exit points of the wheels. A rotary optical encoder attached to the flat wheel measures the longitudinal motion. A computerized data acquisition system monitors these signals and records the tracking behavior of the band. The entry angle ϕ is determined from the ratio of the sideways and longitudinal movements

$$\phi = \frac{\text{sideways movement}}{\text{longitudinal movement}} \tag{5.1}$$

5.2 Equipment Set-up and Accuracy

Accurate geometric set-up of the experimental equipment is critical because a band's tracking behavior depends on the subtle details of the geometry of the wheels and band. For most of the factors such as the wheel profile, band strain, width and overhang, this was a straightforward process. However, the band's tracking behavior was found to be especially sensitive to band backcrown, wheel tilt and wheel cross line. As a result, these factors required extra attention.

The wheel tilt set-up and measurement can be done reliably by controlling the average tilt angle. An imperfect fit or tolerance between the wheel and shaft, the shaft and bearing or a tolerance in the bearing itself can create a misalignment between the axis of the shaft and wheel and the axis of rotation. As a result, the axis of rotation may not coincide with the axis of the shaft and wheel. As the shaft and wheel rotate, their angle changes symmetrically about the axis of rotation. To ensure that the tilt angle coincides with the axis of rotation, the tilt angle was measured by taking the average of the shaft tilt angle over one revolution.

A band can be checked for backcrown by utilizing the geometry of backcrown. When a straight band is turned inside-out the geometry of the band does not change. When a band with backcrown is turned inside-out, its backcrown and curvature are reversed. As a result, backcrown can be detected in a band by comparing the steady state entry angle and tracking position of band in its normal configuration and when it is turned inside-out. A band with backcrown generates different values in each orientation. Bands with significant backcrown were not used in the experiments.

The cross line between the wheel axes can be set to zero by utilizing the tracking effect of cross line. When the cross line is not zero, the geometry of the band and bending moment change when the direction of band rotation is changed. As a result, the steady state entry angle and tracking position of the band also change. Therefore, the wheel axes can be set with zero cross line by adjusting the cross line until the steady state entry angle and tracking position are the same in both directions of band rotation.

Repeated alignment and set-up of the equipment showed the accuracy of the entry angle measurement on a tapered wheel to be within 0.01° or 8%. On a crowned wheel, the stable tracking position was repeatable within 0.005".

In summary, the initial set-up procedure for each experiment was as follows:

1. Securely mount the wheel on the shaft and the shaft in the bearing.
2. Adjust the wheels axes to zero cross line using a machinists level.
3. Mount the desired band on the wheels.
4. Set the band strain.
5. Set the wheel tilt from the average value of four angular shaft positions.
6. Rotate the band until the entry angle reaches steady state or the band tracking position is stable on the wheel. Measure the entry angle or position.
7. Reverse the band rotation until the entry angle reaches steady state or the band tracking position is stable on the wheel. Measure the entry angle or position.
8. Adjust the wheel axes cross line to eliminate the difference in the measured entry angles and positions. Repeat steps 6 and 7 until there is no difference.
9. Release the band and turn it inside-out.
10. Repeat steps 3 to 6.
11. A difference in the measured entry angles or band positions between steps 6 and 10 indicates that the band has backcrown.
12. Rotate the band until the entry angle reaches steady state.
13. Zero the tracking position and longitudinal motion measurements.

5.3 Wheel Taper and Saw Strain, Thickness and Width

A series of three experiments was carried out to examine and validate the basic tracking model of wheel taper, band strain, thickness and width described by equations (4.1) to (4.28). The first experiment examines the complete tracking process of the band including both the transient and stead state behaviors. The second and third experiments examine the effect of band strain and width on the steady state entry angle.

For these experiments, band tracking movement was generated by the profiled wheel with a taper given by

$$f_1(y) = y \tan\left(0.991^0\right) \tag{5.2}$$

The basic equipment set-up and initial position are shown in figure 5.3. After the initial set-up of the equipment as described in section 5.2, the procedure for each experiment was the same.

1. Begin recording the band tracking positions at the entry and exit points of the wheels and the distance traveled by the band.
2. Rotate the band until the entry angle reaches steady state.
3. Stop and note the position and entry angle of the band. These will be used as the initial position and slope for the theoretical model.
4. Continue rotating the steady state tracking band.
5. Stop the band, and change the direction of rotation.

6. Rotate the band as it goes through transient tracking and continue rotating until the entry angle converges to a steady state value.
7. Stop and re-measure the band strain.

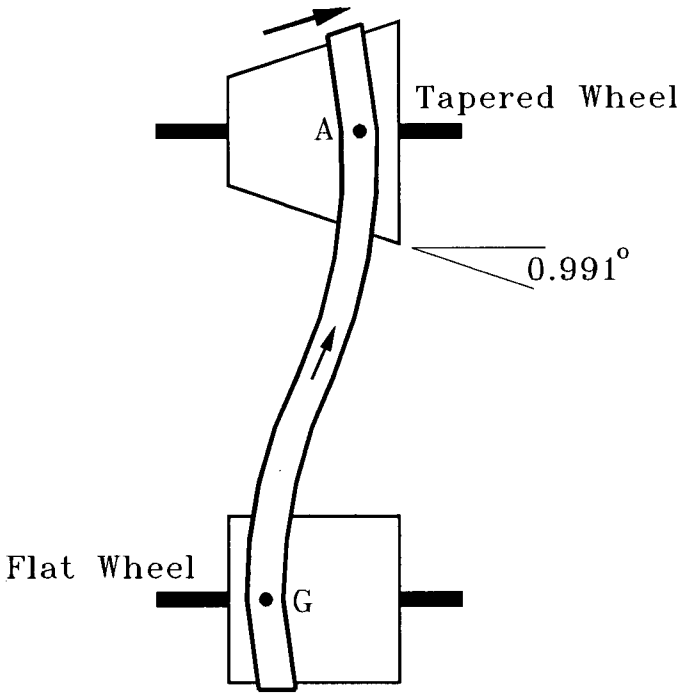

Figure 5.3: Tapered Wheel Experimental Set-up

Tapered Wheel Tracking

Figure 5.4 gives a sample of the results from a typical tapered wheel tracking experiment. The measured band tracking positions on the wheel shown by the solid points closely follow the theoretical data shown by the dashed curves. The left side of the graph, where band travel equals 0 inches, corresponds to step 3 in the above procedure. At 10 inches of travel the band rotation was reversed. This corresponds to step 5. Notice that at 10 inches of travel, the

tracking positions at the exit points lead those at the entry because of the direction of band rotation up to this point. When the direction of rotation is reversed, the process of transient tracking reverses the situation. After 20 inches of travel in the new direction, the entry positions on both wheels now lead those at the exit and the slopes have changed from negative to positive.

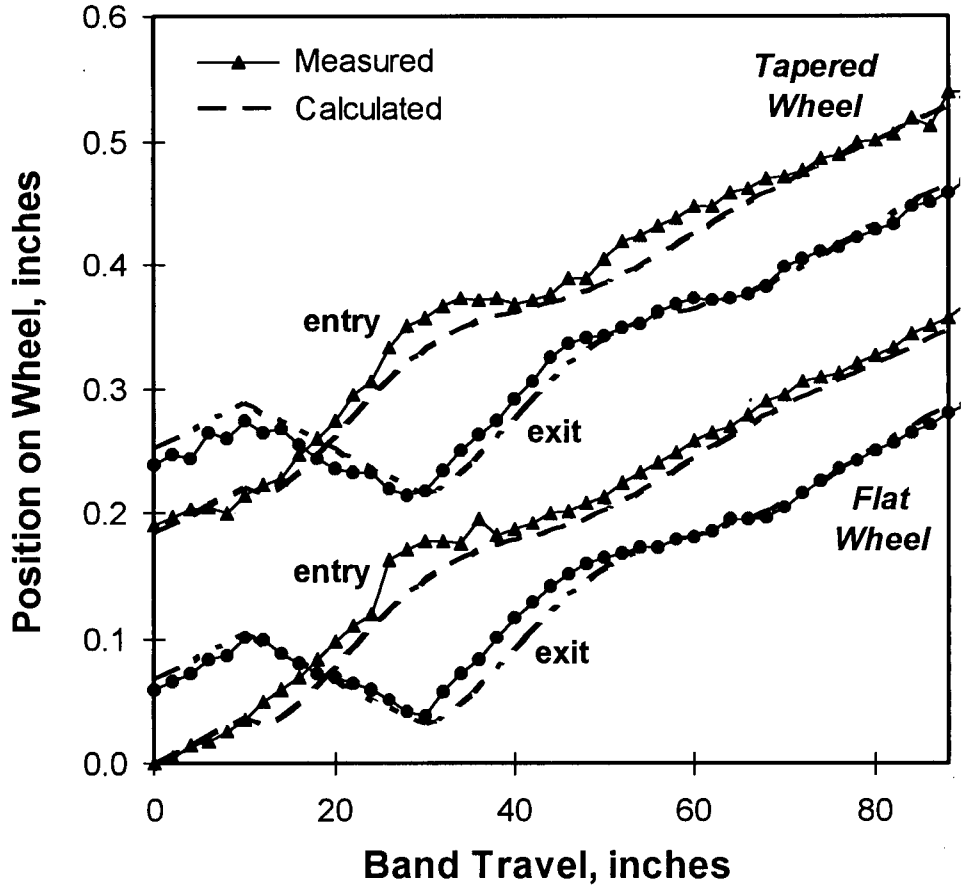

Figure 5.4: Tapered Wheel Tracking
(Strain = 55 lbs, Tilt = 0^0, Width = 0.93")

The slope of the curves in figure 5.4 equal the band angle at the associated entry or exit points. The band position at each wheel exit point lags behind the position at the corresponding entry point. This lag reflects the longitudinal motion required for a point on the band to move around the wheel from the entry to the exit points. A horizontal line drawn between the entry and exit curves has approximately the same length as half the wheel circumference. The lag in position of the band on the flat wheel behind the band on the tapered wheel is the result of the bending moment generated by the tapered wheel. Since the flat wheel does not generate a bending moment, the bending moment generated by the tapered wheel alone drives the tracking motion of the band. The position of the band on the flat wheel follows behind the band position on the tapered wheel. All the curves in figure 5.4 indicate that the entry angle and tracking speed converge to steady state values after about 60 inches of band travel. The measured entry angle converged to a value of 0.20° compared to the theoretical value of 0.21°. The effects of band width and strain on the steady state entry angle will be examined in the next two experiments.

Effect of Band Width on Wheel Entry Angle

Figure 5.5 shows the results of the second experiment on the effect of band width on the steady state entry angle. Again, the measured and theoretical results compare very well. The graphs show that the error between the measured and calculated results is within a 8% range. The effect of band width on entry angle is fairly weak. A 124% increase in band width produces only a 79% increase in entry angle. The effect of band thickness on entry angle is similar in kind, but very much weaker. This latter factor was omitted from the experimental program.

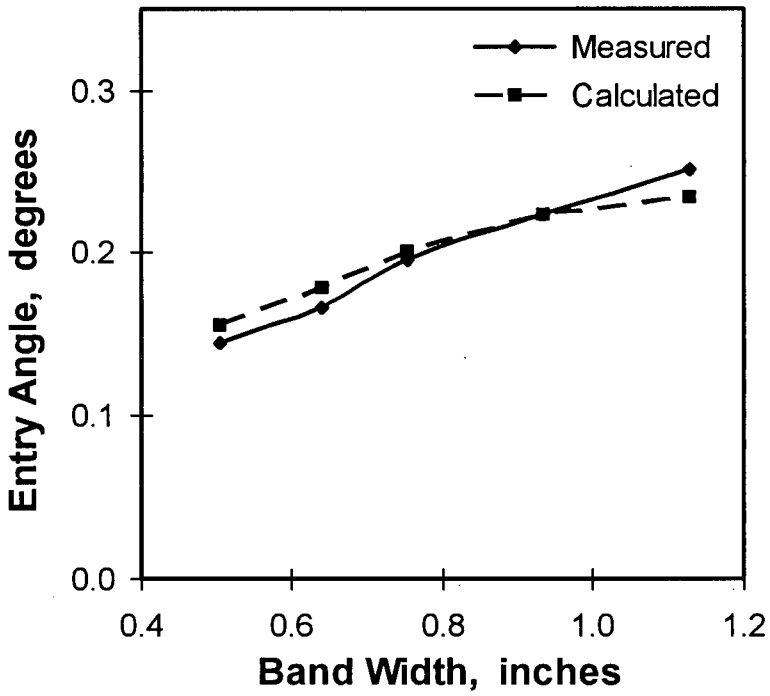

Figure 5.5: Effect of Width on Tapered Wheel Entry Angle
(Strain = 28.3 ksi, Taper = 0.991^0, Tilt = 0^0)

Effect of Band Strain on Entry Angle

Figure 5.6 shows the results of the third experiment on the effect of band strain on the steady state entry angle. Again the measured and theoretical results match very closely. The graphs show that the error between the results is within a 5% range. The trend of both the measured and theoretical results show that strain has very little effect on entry angle. A 90% increase in strain causes only a 17% reduction in entry angle.

The results in figure 5.4, 5.5 and 5.6 show that the basic tracking model of wheel taper, band strain, thickness and width is realistic. The errors between the measured and theoretical results are within the accuracy expected from the equipment.

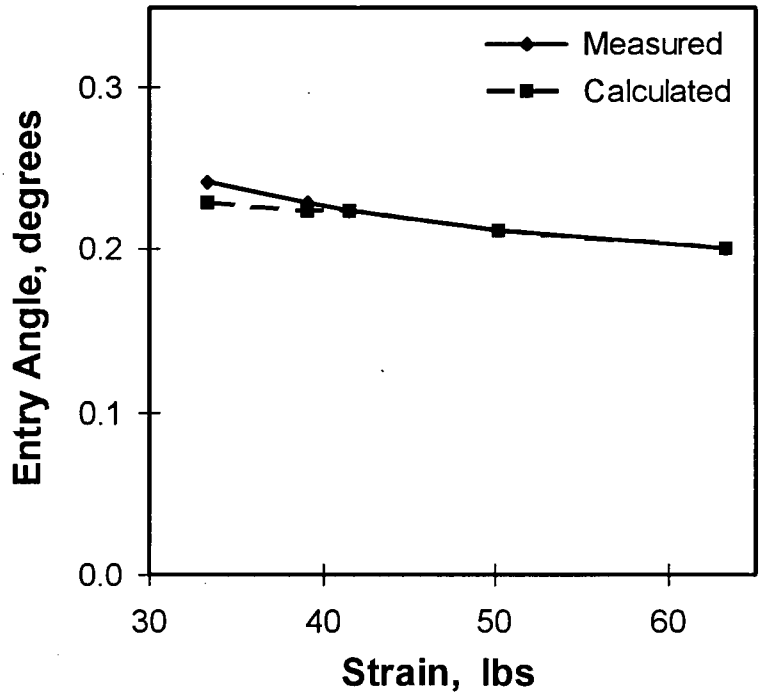

Figure 5.6: Effect of Strain on Tapered Wheel Entry Angle
(Taper = 0.991^0, Tilt = 0^0, Width = 0.93")

5.4 Bandmill Wheel Tilt

An experiment was performed to examine and validate the extension of the basic tracking model to include the effect of wheel tilt. The model was evaluated by comparing the experimental and theoretical effects of wheel tilt on the steady state entry angle. The basic equipment set-up and the initial band position are shown in figure 5.3. The tapered wheel was tilted by various specified amounts. After the initial set-up of the equipment as described in section 5.2, the procedure for each experiment was a follows:

1. Begin recording the band tracking positions at the entry and exit points of the wheels and the distance traveled by the band.
2. Rotate the band until the entry angle reaches steady state.
3. Stop the band and note the position and entry angle of the band. These are defined as the "initial" position and slope for the theoretical model.
4. Set the wheel tilt angle between the axes of the top and bottom wheels.
5. Rotate the band until the entry angle reaches steady state.
6. Stop and re-measure the band strain.

Figure 5.7 shows the effect of wheel tilt on the band steady state entry angle. The measured data shows the same trend as the theoretical data. At the extreme values the theoretical model underestimates the effect of wheel tilt on the entry angle by approximately 0.02° or 7%. The close match between the measured and theoretical results indicates that the tracking model is realistic.

The trend of the curves in figure 5.7 shows that negative wheel tilt increases the entry angle. Conversely, positive wheel tilt decreases the entry angle. At a tilt angle of 1.1° the tracking effect of tilt balances that of taper, causing the entry angle to become zero. A comparison of figures 5.5, 5.6 and 5.7 shows that wheel tilt has a significantly larger effect on the entry angle than that of band strain or width.

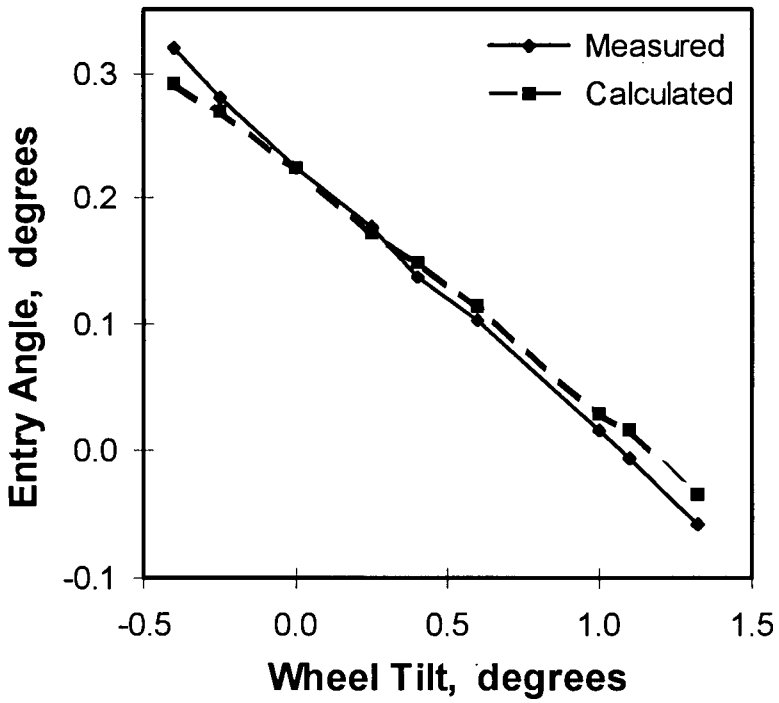

Figure 5.7: Effect of Wheel Tilt on Tapered Wheel Entry Angle
(Strain = 48 lbs, Taper = 0.991^{0}, Width = 0.93")

5.5 Bandmill Wheel Crown and In-feed "Cutting" Force

A series of five experiments was carried out to verify and examine the extension of the tracking model to include the effects of wheel crown and in-feed "cutting" force. In practice, the most common crowned profile used on bandmill wheels is an asymmetric crown [2,3]. Typically, the asymmetric crown has a peak that is not in the center of the wheel, with different profiles on the left and right sides of the peak. This type of crown is shown in figure 5.8. The examination of the tracking behavior of wheel crown begins with a series of three experiments on the general characteristics of symmetric crowned wheels. Two symmetric crowned profiles f_2 and f_3 are shown in figure 5.8. With the general tracking behavior established, a final series of two experiments was carried out to examine the tracking behavior of asymmetric crowned wheels. Asymmetric crown profile f_4 is also shown in figure 5.8.

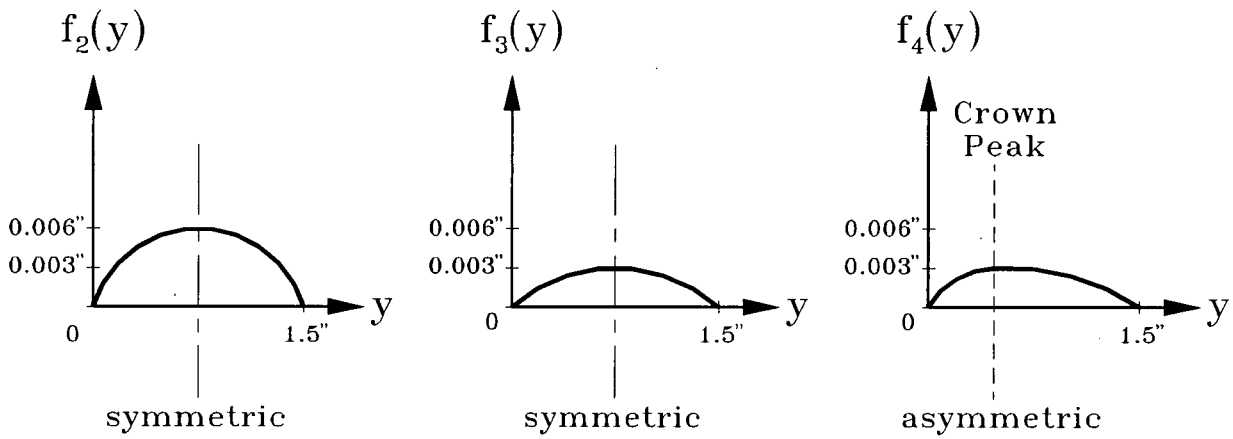

Figure 5.8: Crown Profiles f_2, f_3 and f_4

The five experiments done to investigate the effect of wheel crown are:

1. Examine the complete tracking and self-centering effect of a symmetric wheel crown, including both the transient and steady state tracking behaviors. Since the in-feed "cutting" force can be adjusted independently, it can be used to generate band tracking movement and to test the tracking stability of the bands.
2. Examine the effect of the feed force on the tracking displacement of the band from the center of the wheel crown.
3. Examine the effect of band width on its tracking stability, as measured by the band's displacement from the center of the wheel crown caused by a feed force.
4. Examine the effect of band width on the zero load tracking position on an asymmetric crowned wheel.
5. Examine the tracking stability of the asymmetric wheel crown and how the stability depends on the direction of band displacement on the wheel.

For these experiments the profiled wheel was prepared with crowns f_2, f_3 and f_4

$$f_2(y) = 0.024\, y^2 \tag{5.3}$$

$$f_3(y) = 0.013\, y^2 \tag{5.4}$$

$$f_4(y) = 0.0034\left[(y-0.6484)^5 - 1.7\,(y-0.6484)\right] \tag{5.5}$$

These crowns are shown in figure 5.8. The basic equipment set-up and initial position of the band are shown in figure 5.9. After the initial set-up of the equipment as described in section 5.2, the procedure for each experiment was as follows:

1. Begin recording the band tracking position at the exit point of the profiled wheel and the distance traveled by the band.
2. With no in-feed "cutting" force applied, rotate the band until a stable tracking position on the crown is reached.
3. Stop rotating the band. Use the tracking position of the band at this stopping point as the datum for subsequent tracking measurements as well as the initial position for the theoretical model. The procedure for the fourth experiment ends here.
4. Apply a feed force at the center of the free span of the band between the wheels.
5. Rotate the band until a new stable tracking position on the wheel is reached.
6. Stop the band and remove the feed force.
7. Rotate the band until it returns to the center of the wheel crown.
8. Stop recording the tracking position and longitudinal motion of the band.

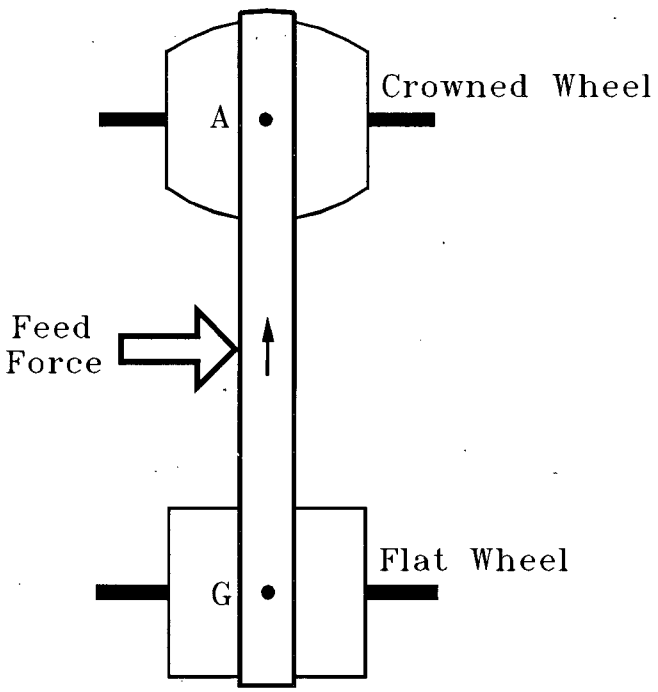

Figure 5.9: Wheel Crown & In-feed "Cutting" Force Equipment Set-up

Crowned Wheel Self Centering

Figure 5.10 gives a sample of the results from a typical crowned wheel transient tracking experiment. The profiled wheel has a crown f_2 given by equation (5.3). The solid jagged line indicates the measured tracking movement of the band. The origin of figure 5.10 corresponds to step 3 of the measurement procedure when the band is at the zero load stable crown center position. The rising curve on the left shows the tracking displacement caused by the application of a feed force (steps 4 & 5). This displacement reached a stable value after about 500 inches of band travel, or five complete rotations of the band. After 600 inches of band travel, the feed force was removed, and the band tracked back to its original stable position at the top of the wheel crown (steps 6-8). The jaggedness in the measured data is caused by unavoidable irregularities along the edges of the 0.002" thick band used in the experiment.

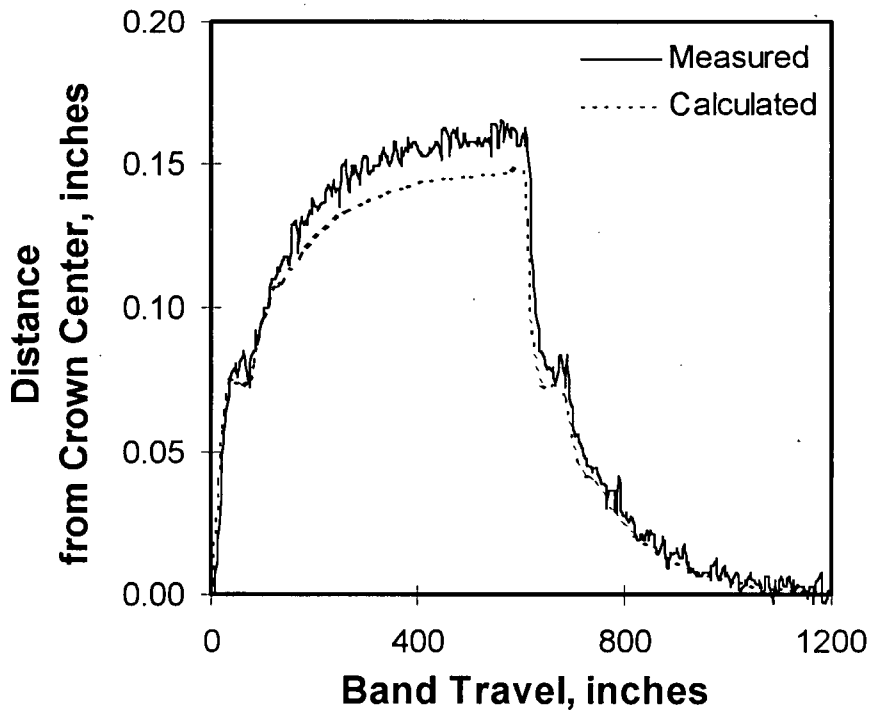

Figure 5.10: Crowned Wheel Transient Tracking
(Feed force = .96 lbs, Crown = f_2, Strain = 55 lbs, Tilt = 0^0, Width = 0.93")

The dotted line in Figure 5.10 shows the calculated tracking response of the band. The theoretical line corresponds very closely with the experimental measurements. The theoretical model successfully predicts the approach to the new stable position from the crown center after the feed force is applied. At this new stable position, the bending moment created by the feed force is balanced by the moment created by the wheel crown. The measured stable tracking position was 0.161" while the predicted position was 0.148".

The theoretical model also successfully predicts the overshoots at 40 inches and at 640 inches of band travel shown in figure 5.10. These overshoots occur because the sudden addition (or removal) of the feed force greatly bends (or straightens) the band at the entry point, and temporarily creates an excessively large entry angle. The band at the wheel entry is able to track off the crown center for half a rotation of the top and then half a rotation of the bottom wheel before the effects of the feed force progresses around to the exit of the flat wheel. At this instant the boundary conditions at the exit of the flat wheel begin to change and the bending moment in the band begins to decrease and change sign. After a few inches of rotation, the band stops tracking away from and begins to head back towards the crown center. Again, after a delay of half a rotation of the top and bottom wheels, the boundary conditions from the new movement appear at the flat wheel exit, the bending moment reverses, the band stops and again begins to track away from the crown center.

Effect of In-feed "Cutting" Force

Figure 5.11 shows the results of the second experiment on the effect of in-feed "cutting" force on the stable tracking displacement from the center of the wheel crown. The wheel crown had profile f_3 given by equation (5.4). Figure 5.11 indicates that the theoretical and experimental results follow the same trends. The theory under-estimates the stable displacement by 12 - 20%. Larger feed forces create larger bending moments which require larger offsets from the wheel crown center to balance. The relationship between the magnitude of the feed force and the distance tracked off the crown center is linear for the parabolic crown profile f_3. This linear relationship can be developed theoretically by substituting equation (5.4) into equation (4.33).

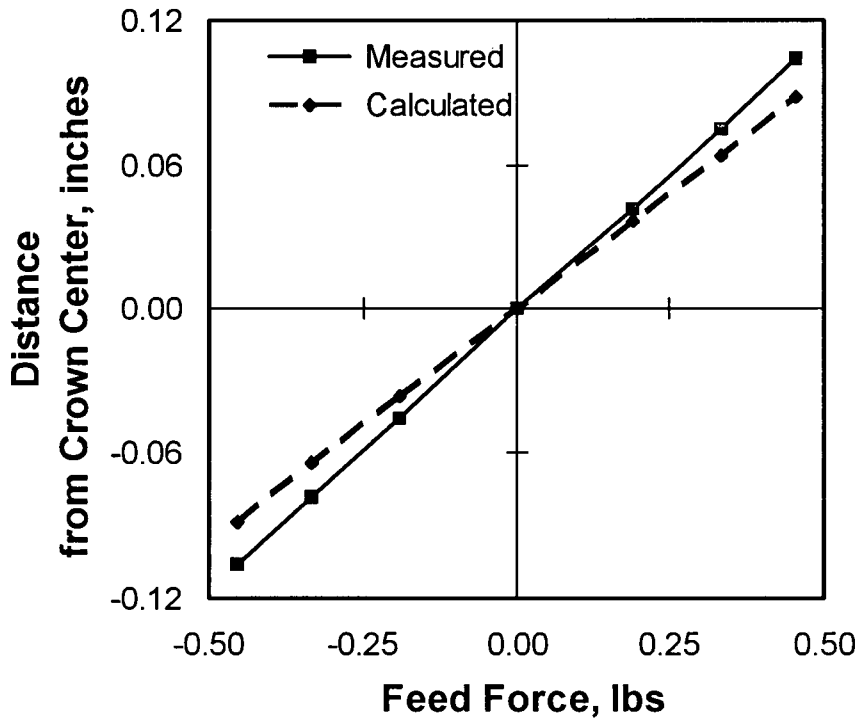

Figure 5.11: Effect of Feed Force on Band Distance from Symmetric Crown Center (Crown = f_3, Strain = 55 lbs, Tilt = 0^0, Width = 1.11")

Effect of Band Width

Figure 5.12 shows the results of the third experiment on the effect of band width on displacement from the center of the wheel crown due to a feed force. Again, the measured and theoretical results show the same trend. The theory underestimates the stable displacement by 0 - 19%. The trend of the graphs show that an increase in the width reduces the distance tracked from the crown center. This occurs because the increased width increases the bending stiffness of the band as explained in section 5.3. This in turn decreases the bending moment and curvature in the band generated by the feed force, and correspondingly reduces the band's offset from the crown center.

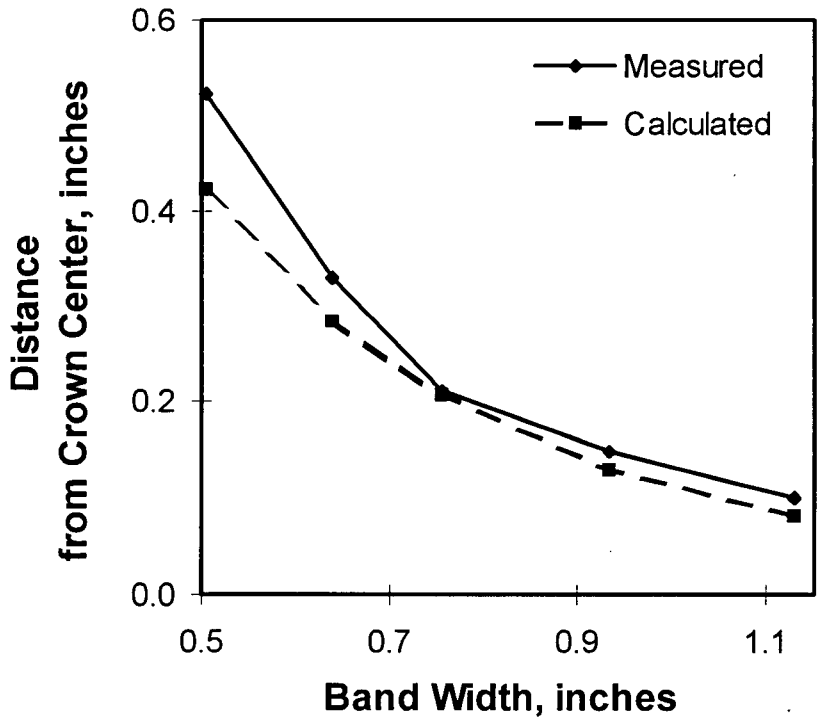

Figure 5.12: Effect of Width on Band Distance from Crowned Wheel Center
(Crown = f_3, Feed force = .73 lbs, Strain = 52 lbs, Tilt = 0^0)

Effect of Band Width on Asymmetric Crown Tracking

Figure 5.13 shows the results of the fourth experiment on the effect of band width on the stable zero force tracking position on an asymmetric crown. This crown profile f_4 is shown in figure 5.8 and is described by equation (5.5). The measured and theoretical results follow the same trend. The difference between the results is in the range of 0.003" for the wider bands to 0.012" for the narrower bands. This error is believed to be due to the difficulty in aligning the wheel axes and setting the backcrown in the bands. In section 5.2, it was explained that the repeatability of the band's stable tracking position was 0.005" due to the difficulty in aligning the wheel axes. It was also mentioned that tracking was particularly sensitive to backcrown. Controlling the backcrown during the manufacture of the smaller width bands

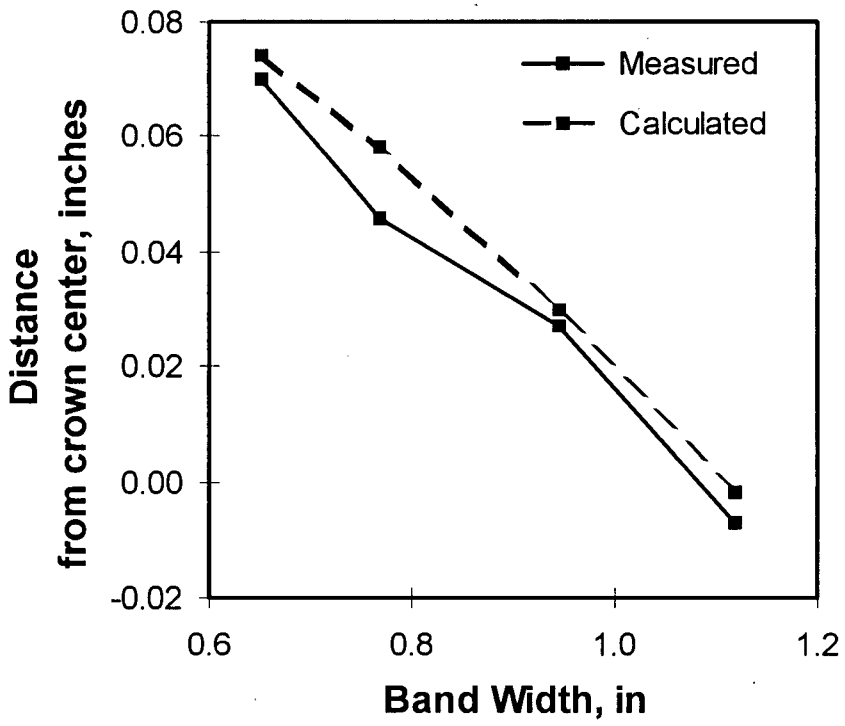

Figure 5.13: Effect of Band Width on the Stable Zero Force Tracking Position
(Crown = f_4, Strain = 20 ksi, Tilt = 0^0)

was more difficult than the larger width bands. As a result, the wheel axes alignment and backcrown combined to create larger errors in the results for the narrower bands.

The dependence of the stable tracking position on the band width can be explained by considering the bending moment in the band. It was shown in section 4.2 that the stress profile across the band matches the profile of the wheel and that the bending moment in the band can be found by integrating the stress profile about the centerline of the band. As explained for the first experiment, the band maintains a stable position on the wheel crown when the bending moment in the band and its entry angle are both zero. When the band is tracking on the center of a symmetric wheel crown, a symmetric stress profile is generated in the band and as a result, the bending moment is zero. Since this symmetry is not affected by the band width, the center of the crown is the stable zero load tracking position for bands of all widths. When the crown is asymmetric, a larger proportion of the band needs to track on the shallower right side of the crown to balance the bending moment generated by the steeper left side, as shown in figure 5.14. As a result, the stable zero load tracking position on an asymmetric crown is always biased towards the shallower side of the crown. When the band width increases as shown in figure 5.14, an even larger proportion of the band needs to rest on the shallower right side to balance the moment from the left. As a result, wider bands tend to track more on the shallower side of the crown. While the narrower bands also track on the shallower side, they tend to track closer to the peak of the asymmetric crown.

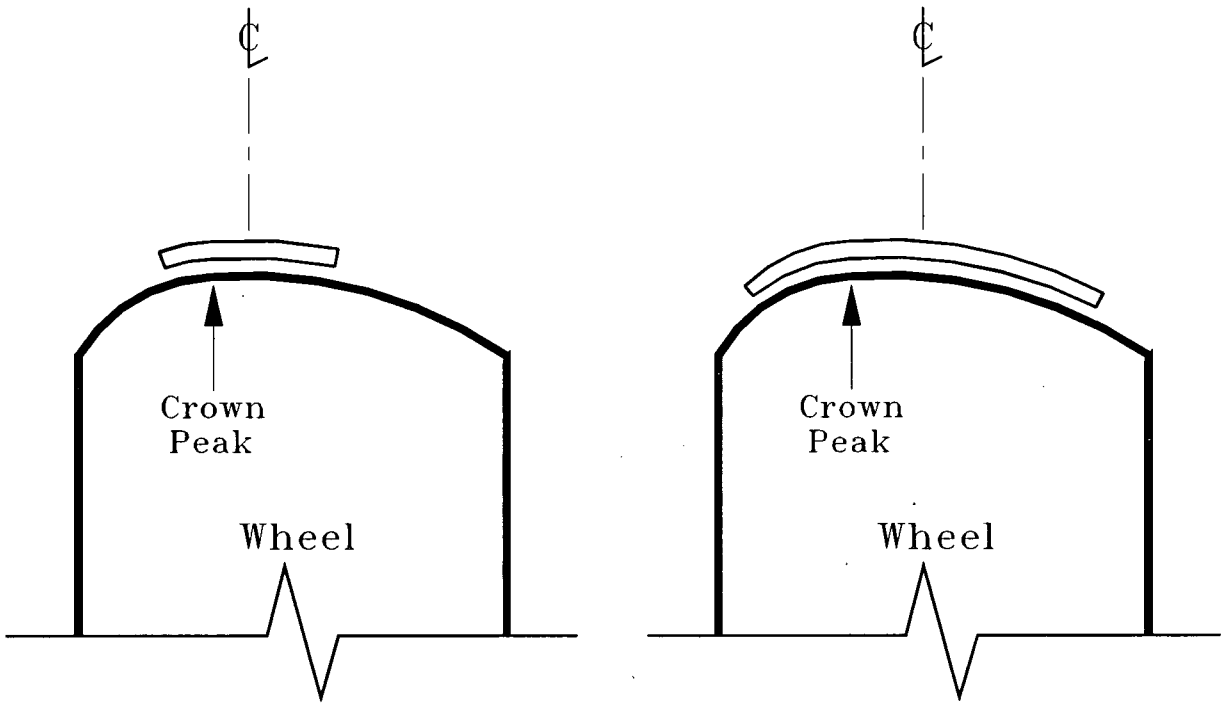

Figure 5.14: Stable Tracking Position on an Asymmetric Crown

Effect of In-feed "Cutting" Force on Asymmetric Crown Tracking

Figure 5.15 shows the results of the fifth experiment on the effect of feed force on the stable displacement from the zero load tracking position on the asymmetric wheel crown profile f_4. The measured and theoretical results show the same trend and again, the theory underestimates the measured results by 0.000" - 0.018" or 0% - 19%. For a non-parabolic crown, the relationship between the feed force and the displacement from the stable zero load tracking position is not linear. When the same force is applied, the displacement of the band onto the steeper side of the crown is less than its displacement onto the shallower side. Therefore, the band has a higher tracking stability in the direction of the steeper side of the crown and a lower stability towards the shallower side. This difference can be explained again

by examining the bending moment in the band. When the force pushes the band onto the steeper left side of the crown, a larger bending moment is generated than when its is pushed the same distance onto the shallower side. As a result, a larger band displacement onto the shallower side of the crown is required to the balance the moment generated by a feed force than when it is pushed onto the steeper side. This difference in tracking behavior also indicates that the tracking stability and behavior of a wheel crown can be adjusted by changing its profile and height.

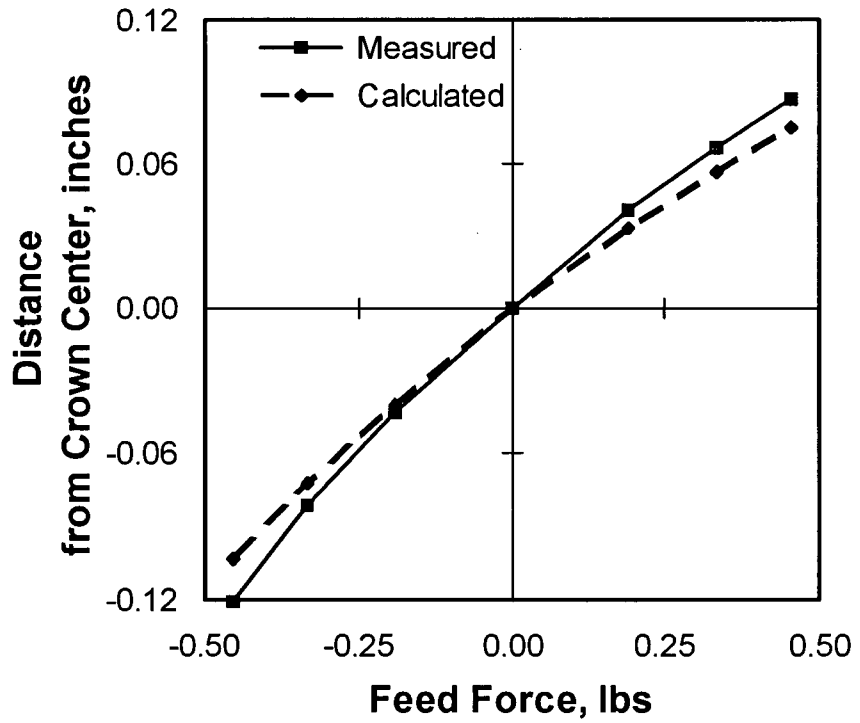

Figure 5.15: Effect of Feed Force on Band Distance from Asymmetric Crown Center (Crown = f_4, Strain = 55 lbs, Tilt = 0^0, Width = 1.11")

The success of the theoretical model in predicting both the general form and details of the band tracking measurements in figures 5.10, 5.11, 5.12, 5.13 and 5.15 confirms that it realistically models the wheel crown and in-feed "cutting" force. The small differences between the theoretical and experimental results is believed to be caused by the band locally buckling under by the applied feed force, as shown in figure 5.16. This local buckling reduces the in-plane stiffness of the band and slightly increases the tracking displacements. This effect reduces with band strain. The higher strain experiments at lower feed forces produced results more closely matching those of the model. Fortunately, in industrial bandsaws, the strains and feed forces tend to be closer to these latter values.

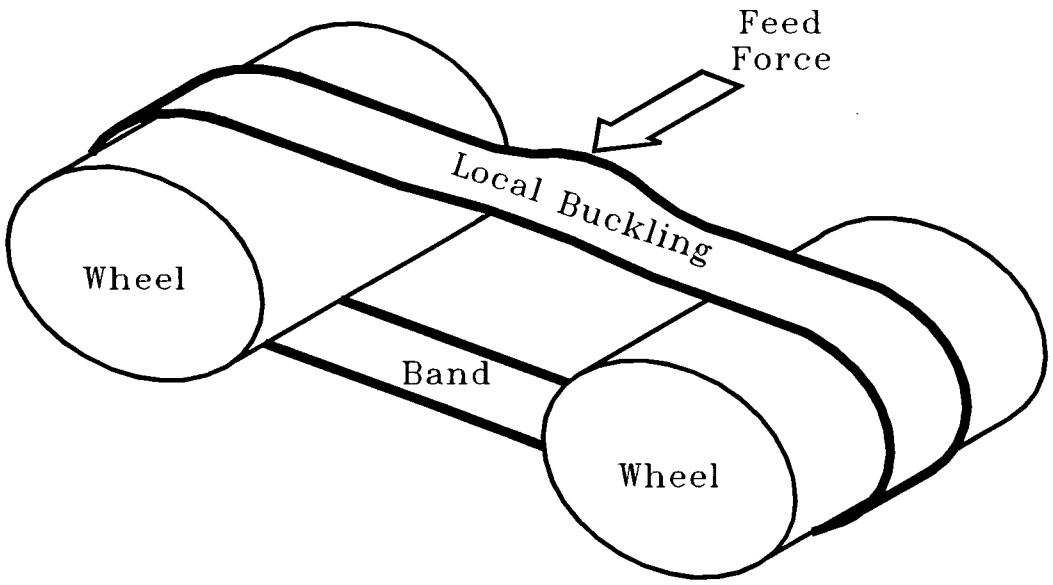

Figure 5.16: Band Buckling from the Feed Force

5.6 Saw Overhang

A series of two experiments was carried out to examine and validate the extension of the tracking model to include the effect of overhang. The first experiment examines the effect wheel tilt on overhang as well as the tracking stability of overhang. The second experiment examines the effect of in-feed "cutting" force on the combined tracking stability of overhang and wheel crown. The tracking stability from the first and second experiments are then compared to determine the benefit of combining overhang with wheel crown.

The basic equipment set-up and the initial positions of the bands are shown in figure 5.17a and b. The profiled wheel shown in figure 5.17b has crown profile f_3 described by equation (5.4).

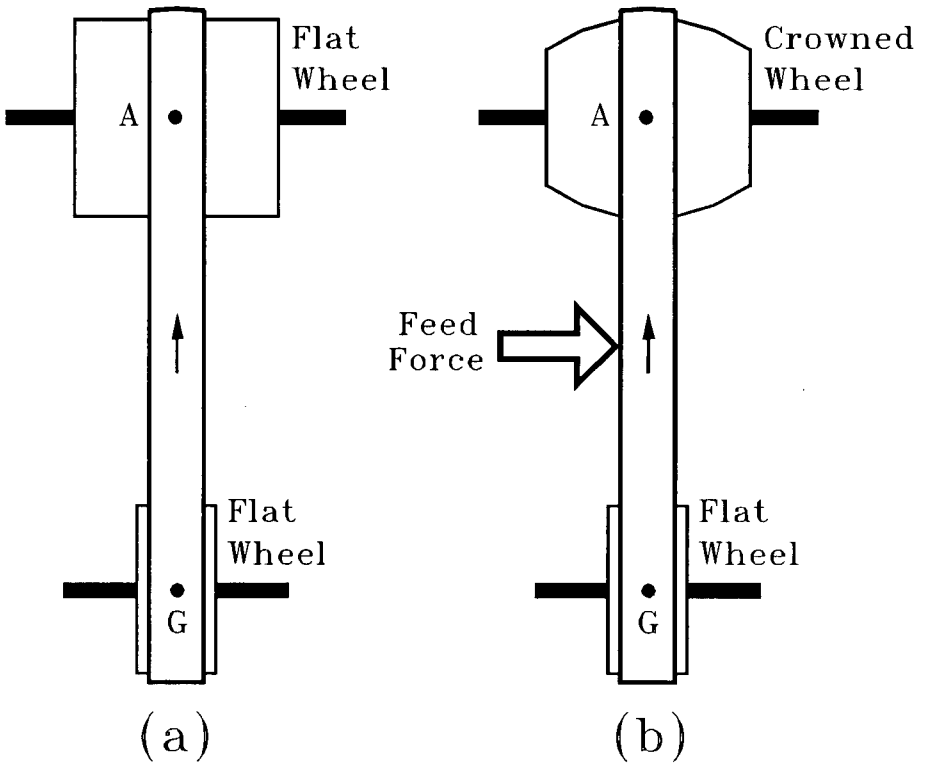

Figure 5.17: Overhang Experimental Set-up

After the initial set-up of the equipment as described in section 5.2, the procedure for the two experiments was the same:

1. Begin recording the band tracking position at the exit points of both wheels and the distance traveled by the band.
2. With no feed force applied, rotate the band until it reaches a stable position on the flat wheel in the first experiment or a stable position on the center of the crowned wheel in the second experiment. In the second experiment, there is no overhang at this point.
3. Stop rotating the band. Use the tracking position of the band at this stopping point as the datum for subsequent tracking measurements as well as the initial position for the theoretical model.
4. In the first experiment, tilt the flat wheel. In the second experiment, apply a feed force at the center of the free span of the band between the wheels.
5. Rotate the band until a stable overhang is reached.
6. Stop recording the tracking position and longitudinal motion of the band.

Effect of Wheel Tilt on Overhang

Figure 5.18 shows the results of the first experiment on the effect of wheel tilt on overhang. Both the measured and theoretical results show that overhang increases with wheel tilt. The difference between the results is initially large but decreases as the wheel tilt and overhang increase. This difference between the results is caused by the low stability of the band when the overhang is small. When the overhang is small, 0.05", the curling of the overhang and the

bending moment generated in the band is also small. When the overhang is increased by 80% to 0.09", the curling and bending moment increased by more than 80%. As a result, when the overhang is small or zero, the band has little tracking stability and a small cross line or wheel tilt creates a large overhang. Although it is conceptually possible to set-up the equipment with zero cross line and tilt, in practice it is extremely difficult. This is shown by the 0.11" measured overhang compared to the 0.00" theoretical overhang at 0^0 tilt. As the overhang increases, the effect of the initial error diminishes in comparison to the effect of overhang, causing the measured and theoretical results to converge.

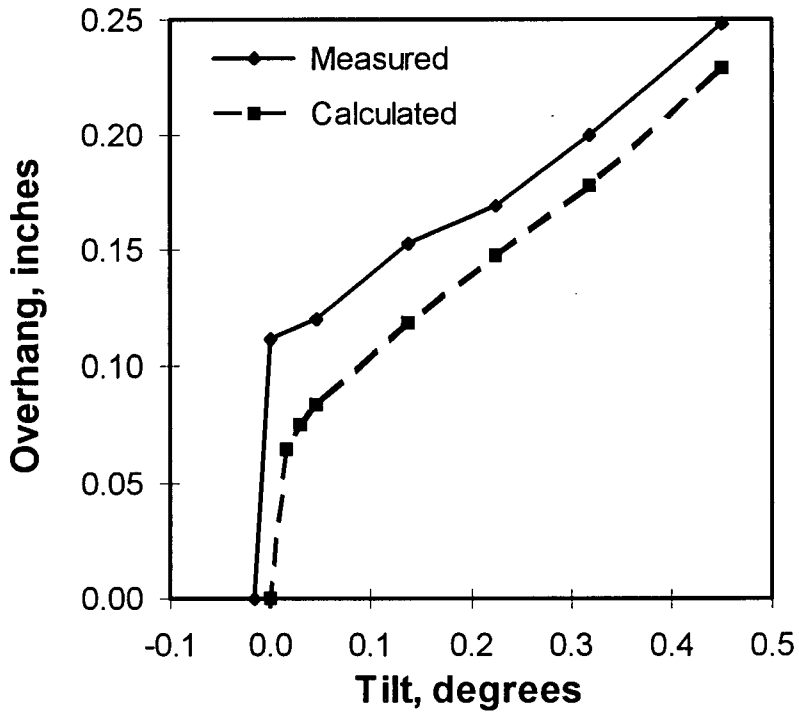

Figure 5.18: Effect of Wheel Tilt on Overhang
(Wheel Profiles = flat, Strain = 55 lbs, Width = 1.11")

Combined Tracking Stability of Overhang and Wheel Crown

The low tracking stability of the band when the overhang is small can be increased by combining overhang with wheel crown. When no feed force is applied to the rotating band shown in figure 5.17b the self centering effect of wheel crown maintains the tracking position of the band at the crown center. When a feed force is applied, the band begins to move off the crown center and develops an overhang on the flat wheel. The bending moments generated by the both the overhang and wheel crown combine to counteract the moment created by the feed force. When the moments balance, the band maintains a stable offset from the center of the wheel crown and a stable overhang.

Figure 5.19 shows the results of the combined band tracking stability of overhang and wheel crown against feed force. The results from the first quadrant of figure 5.11 are shown in figure 5.20 for comparison. Figure 5.20 shows the band tracking stability of only wheel crown against feed force. The effects of overhang and wheel crown can be separated by comparing figure 5.19 to figure 5.20. In figure 5.20 the band displacement from the wheel crown center increases linearly with the feed force. Therefore, the trend of the graphs in figure 5.19 showing that overhang increases with the feed force but levels off as the force increases is due to the tracking effect of overhang. The leveling off of the graphs is caused by the non-linear tracking stability of overhang, as explained for the first experiment.

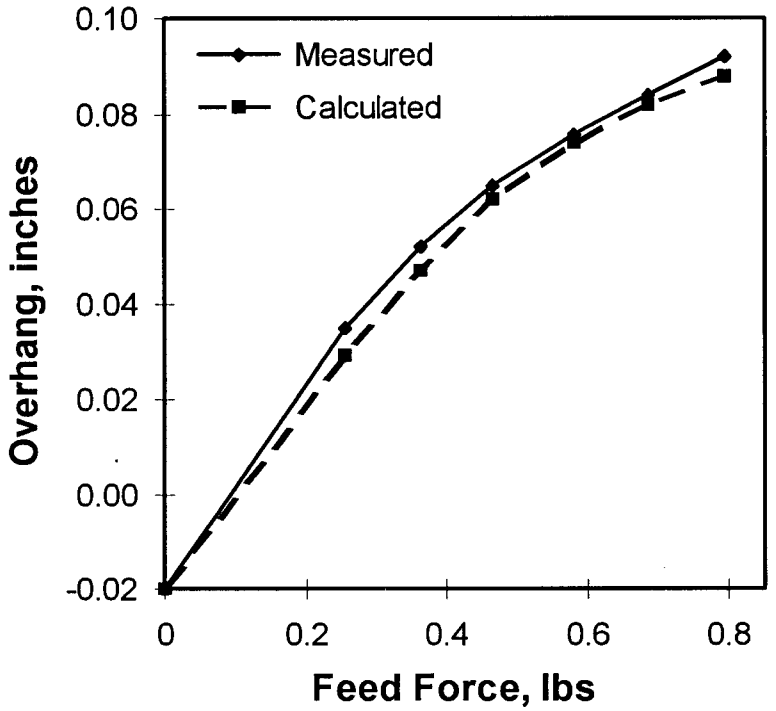

Figure 5.19: Combined Tracking Stability of Overhang and Wheel Crown Against Feed Force (Crown = f_3, Strain = 55 lbs, Tilt = 0^0, Width = 1.11")

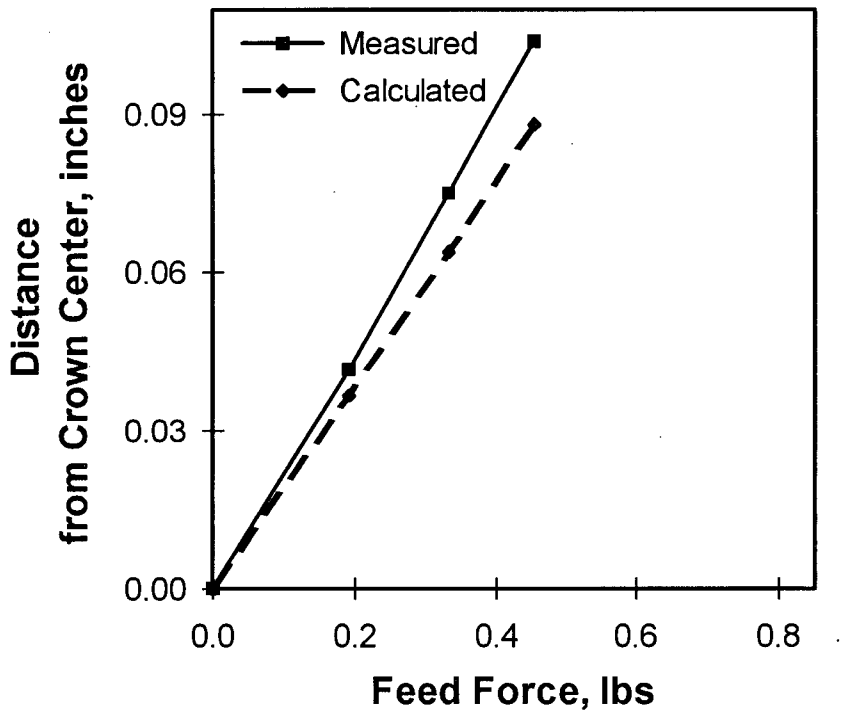

Figure 5.20: Tracking Stability of Wheel Crowned Against Feed Force from Fig. 5.11 (Crown = f_3, Strain = 55 lbs, Tilt = 0^0, Width = 1.11")

A comparison of figures 5.18 and 5.19 shows that when overhang is combined with wheel crown, the band has a high stability at both small and large overhangs. When the tracking stability is from overhang only as shown in figure 5.18, the band is sensitive to misalignment when the overhang is small. When overhang is combined with wheel crown as shown in figure 5.19, the wheel crown increases the tracking stability of overhang. As a result, the band is less sensitive to misalignment.

The measured and theoretical results in both figures 5.18 and 5.19 show the same trend. The difference between the results in figure 5.18 was due to unavoidable small errors in the alignment of the wheel axes as well as to the low tracking stability of the band when the overhang was small. In figure 5.19, the 0.00" - 0.006" or 0% - 20% difference in the measured and theoretical overhang results is believed to be due to the same local buckling phenomenon that was encountered during the wheel crown and feed force experiments, in section 5.5. The close match between the measured and theoretical results indicates that the tracking model of overhang is realistic.

6.0 Conclusions

The theoretical model presented in this thesis identifies and quantifies the main bandsaw and bandmill maintenance and set-up factors that control tracking. The model provides an important tool for the task of improving bandsaw tracking stability. This tool facilitates the improvement of cutting performance and the reduction of required bandmill and sawblade maintenance.

The tracking movement of a band is determined by its entry angle onto each wheel. The band maintains a stable position on a wheel when the entry angle is zero. It tracks sideways across the wheel when the entry angle is non-zero. Tracking movement can be divided into transient and steady state behaviors. Transient tracking occurs when the bending moment and curvature of the band cause the entry angle to change continuously. After a number of band rotations, the transient tracking converges to steady state tracking and the entry angle converges to a steady state value.

Fourteen factors determine the tracking behavior of a band. They are the cutting force, wheel profile, tilt, cross line and coefficient of friction, and the band backcrown, overhang, strain, width, thickness, tension, guides, rotational speed and temperature distribution. These factors determine the bending moment and curvature in the band which control its transient and steady state tracking behavior.

The tracking stability of a band determines its resistance to the cutting force that is trying to push the band off the wheels. A band with a high tracking stability moves very little in response to a cutting force. Tracking stability is determined mainly by the wheel crown profile and overhang. Although the other tracking factors such as strain and width also affect stability, their effect is limited to modifying the stability induced by wheel crown and overhang.

This study concentrated on how six of the above factors affect tracking and stability. The measured and theoretical findings were:

1. **Wheel profile** has a major effect on the tracking behavior and stability of a band. Tapered wheels cause tracking up the taper and crowned wheels cause a self centering effect that gives the band tracking stability to resist the effect of in-feed "cutting" forces. A crown with a more curved profile has a higher tracking stability than a crown with a shallower profile. On an asymmetric crown, a band's stable tracking position is biased towards the shallow portion of the crown. Wider bands track further away from the peak of the crown while narrow bands track closer to the peak. When a band is overhanging the steeper side of an asymmetric crown, as with bandsaw blades, the crown helps to maintain a consistent overhang as the band width decreases. On the other hand, a band running on an asymmetric crown has a lower stability against a feed force that pushes the band onto the wheel than a force in the opposite direction. The sensitivity of a band's tracking stability to the wheel profile indicates that the wheel profile should be designed carefully, machined accurately, and maintained regularly.

2. **Overhang** also has a substantial effect on the tracking behavior and stability of the band. It causes the band to track back onto the wheel. This tracking effect increases with the amount of overhang. When the wheels are flat, overhang gives the band tracking stability, but the stability is high only when the overhang is large. When the wheels are crowned, the overhang adds to the stability of wheel crown. As a result, a band on crowned wheels has a tracking stability that is good when the overhang is small and that increases with overhang.
3. **Wheel tilt** has a significant effect on the tracking behavior of a band. The band tracks from the higher portion of the wheel axis down towards the lower portion. The entry angle and tracking rate increase with the tilt angle.
4. **Width** increases the tracking stability of a band by increasing the tracking effect of wheel profile and the band's resistance to the cutting force.
5. **Band strain** has only a small effect on the tracking behavior of a band. It slightly reduces the entry angle created by wheel taper.
6. A **cutting force** causes tracking in the direction of the force. The band maintains a stable position when the tracking effects of the wheel crown or overhang balance that of the force.

The close similarity of the measured and theoretical results indicate that the theoretical model can be used as a valuable foundation for practical design and for studies of bandsaw tracking on industrial bandsaw machines. The model can now be applied to find an optimum wheel crown profile. It may be possible to modify existing profiles to achieve higher bandsaw

tracking stability while at the same time reducing the amount of tensioning. This should have the desired results of improving cutting performance while at the same time reducing bandmill wheel and sawblade maintenance.

In summary, the main contributions of this study are:

1. Application of the belt tracking mechanism identified by Swift [8] and the geometric model of circular saw hunting identified by Schajer [9] to bandsaw blades.
2. Identification of the transient tracking process and its convergence to steady state tracking.
3. Identification of the fourteen factors which affect bandsaw tracking and the placement of them into a logical framework.
4. Identification of the two primary factors which affect bandsaw tracking stability. They are wheel crown and overhang.
5. Development of a transient tracking model of wheel taper, wheel tilt, band strain, band thickness and band width that converges to Swift's [8] steady state model. Extension of the tracking model to include the tracking effects of cutting force, wheel crown, and band overhang. This included the development of a new model of overhang based on Sugihara's [6] and Taylor's [11] cylindrical shell assumptions.
6. Experiment measurement of the details of band transient tracking including the band displacement overshoot that occurs on a crowned wheel on when the cutting force is initially applied and removed.
7. Measurement and comparison of the tracking stability of wheel crown and overhang.

7.0 Work for Future Projects

To continue with the goal of increasing sawing performance and reducing bandmill wheel wear and the required sawblade maintenance through a study of bandsaw tracking, the theoretical tracking model should be applied to an industrial bandsaw machine. A full size machine is required for the next four steps. They are:

1. Perform experiments to quantify the benefit of improving bandsaw tracking stability on cutting accuracy, bandmill wheel wear and sawblade maintenance. It is believed that low stability or excessive in-plane "front-to-back" motion impairs cutting accuracy by causing the teeth to curl out of the plane of the sawblade during cutting. Excessive tracking movement is also believed to increase the wear between the sawblade and wheel as well as the heat that the wear generates. As a result, low stability would also increase the maintenance required for the sawblade and wheels. Tensioning is a time consuming part of daily bandsaw maintenance. Since tensioning is a tracking factor, a study of tracking may provide a means of reducing the amount of required tensioning.
2. Reaffirm the experimental results shown in section 5 by repeating the experiments on an industrial bandsaw machine. It is anticipated that on an industrial machine the correspondence of the measured and theoretical results will further improve. A thicker and wider sawblade under higher strain will have a higher stiffness and as a result, reduce the local buckling problems caused by the in-feed "cutting" force.
3. Extend the tracking model to include the effects of wheel axis cross line, out-of-plane cutting force, saw guides, backcrown and tensioning and then experimentally verify

each extension. In section 5 it was shown that tracking is very sensitive to cross line, and as a result, may have affected some of the measurements. The addition of the cross line to the model will allow a study of the sensitivity of tracking to cross line as well as allow the effect of cross line to be included in the results. The addition of an out of plane "cutting" force, saw guides, backcrown and tensioning to the tracking model allows their tracking effects to be examined and makes the model a closer representation of a industrial bandsaw machine.

4. Apply the theoretical tracking model to improve the tracking stability of the bandsaw and reduce the required tensioning. One possible way to accomplish this is by redesigning the wheel profile. It was explained earlier that tensioning allows the edges of the sawblade to contact the wheel firmly. A redesign of the wheel profile should allow the edges of the saw to contact the wheel with less tensioning while at the same time improving the tracking stability of the sawblade. This should have the desired effect of improving cutting performance while at the same time reducing wheel wear and sawblade maintenance.

References

1. Brown, T.D. "Quality Control in Lumber Manufacturing." Miller Freeman Publications, San Francisco, CA. 1982.

2. Williston, E.M. "Saws Design Selection Operation Maintenance." Miller Freeman Publications, San Francisco, CA. 1989.

3. Quelch, P.S. "Armstrong Saw Filer's Handbook." Armstrong Manufacturing Company. Portland, Oregon. 1966.

4. Cumming, J. D. "Control of Band Saw Behavior." Proceedings 3rd Wood Machining Seminar. UC Forest Products Laboratory. Richmond, CA. pp.29-37. 1967.

5. Kuno, R. and Doi, O. "Stretching of Band Saw Blades. I. Running Stability of Saw Blades." Bulletin of the Faculty of Engineering, Hokkaido University. Vol.10, pp.53-71. 1954.

6. Sugihara, H. "Theory of Running Stability of Band Saw Blades." Proceedings 5th Wood Machining Seminar. UC Forest Products Laboratory. Richmond, CA. pp.99-110. 1977.

7. Chardin, A. "Displacement of Band Saw Blades on Wheels: Comparison Between a 5-foot and an 8-foot Band Saw." Proceedings 7th Wood Machining Seminar. UC Forest Products Laboratory. Richmond, CA. pp.183-192. 1982.

8. Swift, H. W. "Cambers for Belt Pulleys." Proceedings Institution of Mechanical Engineers, London. Vol.122, pp.627-659. 1932.

9. Schajer, G.S. "Guided Saw Hunting." Forest Products Journal. Vol. 38, No. 4, pp.47-50. 1988.

10. Renner, E.J. "Belt Pulley Crown." Machine Design Journal. September 29. pp.106-109. 1960.

11. Taylor J. "The Effect of Bandsaw Stresses on Blade Stiffness and Cutting Accuracy." Ph.D. Thesis, University of British Columbia, Vancouver, B.C. 1993.

12. Chardin, A. "Displacement of Band Saw Blades on Wheels: An Experimental Approach." Proceedings 6th Wood Machining Seminar. UC Forest Products Laboratory. Richmond, CA. pp.209-221. 1979.

13. Chardin, A. and Sales, C. "Bandsaw Blade Stability: Effects of Wheel Geometry and Tensioning." Proceedings 8th Wood Machining Seminar. UC Forest Products Laboratory. Richmond, CA. pp.405-415. 1986.

14. Sales, C. G., Guitard, D. Fournier, M. and Garin, D. "Recent Advances in Sawing Tropical Woods: Bandsaw Blade Behavior and Industrial Applications." Proceedings 9th Wood Machining Seminar. UC Forest Products Laboratory. Richmond, CA. pp.35-54. 1988.

15. Rivat, J.M., Sales, C. and Martin, P. "Bandsaw Performance Improvement - I - Theoretical and Experimental Aspects of an Industrial Bandsaw Blade Behavior During No-load Running." Proceedings of the 12th International Wood Machining Seminar. Kyoto, Japan. pp.357-366.

16. Wong, D.C. and Schajer, G.S. "Factors Affecting Bandsaw Tracking." Wood Machining Institute. Seattle, WA. 1995.

17. Wong, D.C. "Bandsaw Tracking Stability for Improved Cutting Accuracy." Unpublished paper. 26 pp. 1996.

18. Taylor, J. "An Investigation into Factors Affect the Cutting Bias in Bandsaws." Proceedings Sawtech 95'. Wood Machining Institute. Seattle, WA. 1995.

19. Kirbach, E. "Problems and Solutions in Maintenance and Operation of Band Saws" Forintek Canada Corporation Report. Vancouver, B.C. 25 pp. 1986.

20. Timoshenko, S. "Strength of Materials. Part II. Advanced Theory and Problems." Third Edition. D. Van Nostrand Company Inc., Princeton, New Jersey. 1958.

21. Timoshenko, S. "Strength of Materials. Part I. Elementary Theory and Problems." Third Edition. D. Van Nostrand Company Inc., Princeton, New Jersey. 1958.

22. Timoshenko, S. And Woinowsky-Krieger, S. "Theory of Plates and Shells." Second Edition. Mcgraw-Hill Book Company, Toronto. 1959.

23. Roark, R.J. and Young, W.C. "Formulas for Stress and Strain, Fifth Edition." Mcgraw-Hill Kogakusha Ltd., Tokyo, Japan. 1975.